MULTIPLEXING IN NETWORKS AND DIFFUSION

ARUN G. CHANDRASEKHAR[‡], VASU CHAUDHARY[§], BENJAMIN GOLUB[§], AND MATTHEW O. JACKSON[†]

Abstract. Social and economic networks are often multiplexed, meaning that people are connected by different types of relationships—such as borrowing goods and giving advice. We make three contributions to the study of multiplexing. First, we document empirical multiplexing patterns in Indian village data: relationships such as socializing, advising, helping, and lending are correlated but distinct, while commonly used proxies like ethnicity and geography are nearly uncorrelated with actual relationships. Second, we examine how these layers and their overlap affect information diffusion in a field experiment. The advice network is the best predictor of diffusion, but combining layers improves predictions further. Villages with greater overlap between layers (more multiplexing) experience less overall diffusion. This leads to our third contribution: we develop a model of diffusion in multiplex networks. Multiplexing slows the spread of simple contagions, such as diseases or basic information, but can either impede or enhance the spread of complex contagions, such as new technologies, depending on their virality. Finally, we identify differences in multiplexing by gender and connectedness. These have implications for inequality in diffusion-mediated outcomes such as access to information and adherence to norms.

Keywords: networks, social networks, multiplex, multi-layer, diffusion, contagion, complex contagion

JEL codes: D85, D13, L14, O12, Z13

Date: December 13, 2024.

[‡]Department of Economics, Stanford University; NBER; J-PAL.

[†]Department of Economics, Stanford University; Santa Fe Institute.

[§]Department of Economics, Northwestern University.

Yann Calvó López provided exceptional research assistance. We thank Paul Goldsmith-Pinkham for helpful conversations. Research was supported by NSF grants SES-1629328 and SES-2018554. Chandrasekhar acknowledges the Alfred P. Sloan Foundation for financial support.

1. Introduction

People maintain many different types of relationships—for example, collaborating with colleagues at work, relying on friends and acquaintances for assistance and advice, and engaging in the borrowing and lending of money or goods with family and friends. A given pair of people can have multiple such relationships. For example, people interact both in-person and online, and while some pairs are linked in both offline and online networks, the overlap between these networks is far from complete (Boccaletti et al., 2014). Similarly, college students' partners in social activities overlap with, but also differ from, the people to whom they turn during times of stress or for academic collaboration (Morelli et al., 2017; Jackson et al., 2024).

The coexistence of distinct types of relationships among the same population is known as *multiplexing* (see, e.g., Kivela et al. (2014)), and the interdependence of different types of relationships has been discussed since Simmel (1908). Although numerous case studies have examined multiple relationships, many basic questions remain open concerning the empirical patterns of multiplexing in social and economic relationships, as well as how multiplexing impacts outcomes of interest such as information diffusion.

In this paper, we make three contributions.

First, in Section 2, we report results from unsupervised statistical analyses examining correlation structures across network layers in two large datasets. We document both significant correlation between different network layers (types of relationships) and meaningful differences in their patterns. Without properly accounting for the multiplexed nature of relationships, researchers may arrive at misleading conclusions about peer effects and influence. We show that layers of informational relationships, financial relationships, and social relationships, among others, exhibit strong correlations in a sample of 143 villages in Karnataka, India, comprising nearly 30,000 households (Banerjee et al., 2013, 2019, 2024b). Although these layers are correlated, we show that they display distinct patterns and differ in density and other network statistics. We also show that proxies for social relationships that are commonly used in the peer effects literature, such as geographic proximity or co-ethnicity (in our data, being members of the same *jati*, or subcaste), are nearly orthogonal to the other layers. This suggests that relational variables constructed based on geographic or ethnic covariates may not be accurate surrogates for actual social and economic relationships.

Second, we use supervised statistical methods to show that distinctions among layers are substantively important for the study of economic outcomes, specifically the diffusion of information or behaviors. While one might have expected little difference in the predictive power of different network layers for outcomes of interest, we find that the

different layers contain distinct information and combine to form a nuanced overall picture. Using data from a randomized controlled trial of information diffusion, we show that some layers are more predictive of diffusion than others—with an "advice" layer standing out—and moreover that using a suitable combination of layers yields predictions significantly better than those based on any single elicited layer. A combination of layers also affords better predictions than using the union or intersection of layers. These findings indicate that the elicited layers are not simply noisy observations of a latent one-dimensional relationship, instead containing information richer than any natural one-dimensional summary.

An additional finding regarding ethnic links further supports the point that links are most usefully viewed as multi-dimensional. We show that, while the jati layer is the least predictive of diffusion and not a good substitute for actual relationships, combining it with other layers significantly improves diffusion predictions. Thus, although jati is not a good substitute for elicited network data,[1] it can serve as a valuable complement.

We close Section 2 with an important empirical observation: villages that are more multiplexed (have more strongly correlated layers) experience less diffusion. This correlation between layer overlap and diffusion sets the stage for our theoretical analysis.

Motivated by the fact just presented, Section 3 develops our third main contribution—new theoretical results on how multiplexing relates to diffusion. First, we examine how the degree of multiplexing affects a standard diffusion or contagion process in which a person may be infected/informed by any single infected other (called *simple* contagion). We introduce a definition capturing what it means for an individual to be unambiguously more multiplexed in one multiplex network than another. We show that when such a comparison can be made, the more multiplexed individual is less likely to become infected for any given probability of neighbor infection. Building on this basic result, we demonstrate that in a standard SIS (Susceptible-Infected-Susceptible) simple contagion model, the steady-state infection rate decreases as individuals become more multiplexed. These results can be summarized by saying that multiplexing impedes simple diffusions. We then develop a theory examining how multiplexing impacts *complex* diffusion processes—ones in which people only become infected or adopt a new behavior/practice if they experience sufficiently many interactions with infected others. Here we show that multiplexing can either enhance or impede diffusion, depending on the virality of the process. The nonmonotonicities identified by our theory reveal that multiplexing has subtle implications for theories for threshold contagion models.

[1]As we discuss below, using the jati variable drastically over-predicts links within jati, and under-predicts them across jati. One conjecture as to why the jati layer helps in predicting diffusion is that patterns of information passing on the network are related to jati.

We close the paper in Section 4 with observations about how multiplexing varies with individual characteristics and some implications for issues of inequality. We find that women's networks display significantly more multiplexing than men's networks, and that multiplexing correlates negatively with the number of connections a person has. Given our theoretical and empirical evidence showing how multiplexing can impede simple diffusions, this suggests that multiplexing functions as a channel limiting women's exposure to information. More broadly, demographic differences in multiplexing imply that network-mediated contagions work differently in different subpopulations—a rich topic that we believe deserves further study.

The literature on multiplex networks has begun to grow in the last decade (Contractor et al., 2011; Boccaletti et al., 2014; Kivela et al., 2014; Dickison et al., 2016; Bianconi, 2018). The recognition that people are involved in different types of relationships dates to some of the original works on network analysis (e.g., Simmel (1908)), and instances of the fact that different layers can serve different roles have been analyzed over time (Wasserman and Faust, 1994; Becker et al., 2020). More recent studies have shown that distinguishing between different networks and tracking their interplay can be important in understanding cooperative behavior (Atkisson et al., 2019; Cheng et al., 2021) as well as understanding play in network games and targeting policies to influence it (Walsh, 2019; Zenou and Zhou, 2024).

Our contributions to the literature on multiplex networks are threefold.

First, we provide some of the first detailed statistical analyses of how multiple layers relate to each other in empirical social networks. Second, we show how different layers—as well as the level of correlation between layers—predict diffusion outcomes. This suggests that unidimensional theories of diffusion and contagion can miss important factors that determine the extent of diffusion. Third, we develop a new theoretical analysis of how correlation between layers impacts diffusion, which provides a basis for interpreting our empirical observations about multiplexing and diffusion.

While some theoretical work has examined simple (Hu et al., 2013; Larson and Rodriguez, 2023) and complex (Yağan and Gligor, 2012; Zhu et al., 2019; Kobayashi and Onaga, 2023) diffusion on multiplexed networks, previous analyses have focused on independently distributed layers. Such diffusion models are a more direct extension of diffusion on one layer and the proofs in the existing literature leverage that fact. Our analysis examines how changes in layer overlap affect diffusion. In addition—and in contrast to prior models—our model also allows for interactions (such as conversations or information transmissions) to be correlated across layers, even conditional on links.

Our findings on the impact of multiplexing on diffusion can help inform a nascent and important literature on the incentives to form multiplexed networks (Billand et al., 2023; San Román, 2024). For example, a series of empirical studies on rural developing economies emphasize the role social networks play in risk-sharing arrangements (Townsend, 1994; Fafchamps and Gubert, 2007; Ambrus et al., 2014). This raises a fundamental question: If individuals primarily organize their relationships around risk-sharing and multiplex other relationships on top of the risk-sharing relationships, how might these structures affect the diffusion of new information or technologies? Both our empirical findings and theoretical results shed light on this issue.

2. Multiplexing in the Data

2.1. **Two Data Sets.**

We study two different data sets of multiplex networks in a total of 143 villages, both from the state of Karnataka, India, covering a total population of nearly 30,000 households.

2.1.1. *The Microfinance Village Sample.* The first dataset that we use, which we refer to as the "microfinance village sample," comes from network data collected in Wave II of a study of 75 villages (Banerjee et al., 2013, 2024b). In 2012, that study obtained a complete census of the 16,476 households across these 75 villages. From 89.14% of these households, it then collected detailed socio-economic network data, described below. (This means that the study obtained information on 98.8% of the links.[2])

The study collected information on various types of interactions for each respondent, spanning social, financial, informational, kinship, and religious networks. The surveys asked respondents about the following types of relationships, each listed with an abbreviated label that we use from now on to refer to it:

(1) social: to whose home does the respondent go and who comes to their home, as well as which close relatives live outside their household;
(2) kerorice: from whom does the respondent borrow kerosene/rice and to whom does the respondent lend these goods;
(3) advice: to whom does the respondent give information/advice;
(4) decision help: to whom does the respondent turn for help with an important decision;
(5) money: if the respondent suddenly needed to borrow 50 rupees for a day, to whom would they turn, and who would come to them with such a request;

[2]Given our focus on undirected graphs, we elicit a link as long as at least one of the two households on either end is sampled. With 89.14% of the households being sampled, for two arbitrary nodes i and j, we compute $\mathrm{P}(i \text{ or } j \text{ in sample}) = 1 - (1 - 0.89)^2 = 0.9879$.

(6) temple: if the respondent goes to a temple, church, or mosque, who might accompany them;
(7) medic: if the respondent had a medical emergency alone at home, whom would they ask for help in getting to a hospital.

Additionally, we have information on the jati (subcaste) and GPS coordinates for each household. This allows us to construct jati networks (in which pairs from the same subcaste are linked) and geographic networks, whose edges are labeled by distance in physical space. Variables of these types have been used as proxies for social networks in prior studies (e.g., Sacerdote, 2001; Fafchamps and Gubert, 2007; Munshi and Rosenzweig, 2009).

2.1.2. *The Diffusion RCT Sample.* The second dataset that we use, which we call the "RCT village sample," contains multiple network layers from a set of 68 different villages collected by Banerjee et al. (2019).

The network data was collected in a manner similar to that of the Microfinance Village Sample. The surveys elicited information about the following layers:

(1) social: to whose home does the respondent go and who comes to their home to socialize;
(2) kerorice: from whom does the respondent borrow kerosene/rice or small amounts of money and to whom does the respondent lend these goods;
(3) advice: to whom does the respondent give information/advice;
(4) decision: to whom does the respondent turn for help with an important decision.

While we have jati information for the RCT villages, we lack GPS data for this sample.

In addition, we have the data from a randomized controlled trial (RCT) studying diffusion in these villages, which is the subject of Banerjee et al. (2019). This RCT provides cleanly identified estimates of diffusion, allowing us to examine how diffusion varies with different aspects of multiplexed networks. Specifically, in each village, the study seeded either 3 or 5 individuals (determined uniformly at random) with information about a promotion. Villagers could obtain a non-rivalrous chance to win either cash prizes or a mobile phone by calling in to register for the promotion.[3] Registered callers were visited a few weeks later and received a reward.[4] Thus, the study experimentally

[3]In particular, they had to dial the provided promotional number and leave a "missed call." This was a call that we registered but did not answer and was free for the participant to make, which was a standard technique for registration at the time.
[4]The individual rolled a pair of dice and received INR 25 $\times$ the number rolled. This yielded cash prizes of amounts ranging from INR 50 (for a 2) to INR 275 (for an 11). A roll of 12 was rewarded with a cell phone worth INR 3000. The expected value of the prize was INR 255, which was more than half of a day's wage in the area.

induced the diffusion of a non-rivalrous, valuable piece of information. The outcome variable of interest is the number of households that registered. There was exogenously randomized variation in the position of the random seeds in the network, and more central seeds caused larger diffusions. We use our data on multiplexing to examine how diffusion depends on the network statistics of the seeds in various network layers, used individually and in combination, and on network multiplexing levels.

2.2. **The Layers and Multiplexing Patterns.**

We begin with some descriptive statistics on the network layers. A link is present in a given layer if either household named the other household in one of the questions in that category (e.g., we code a kerorice link if either household reports borrowing kerosene or rice from or lending it to the other household). In terms of notation, we define a multi-layered, undirected network for each village v,[5] for layer $\ell = 1, \ldots, L$, with $g^{\ell}_{ij,v} = 1$ if either household i or j reported having a relationship of type ℓ. We add another layer where i and j are linked if they belong to the same jati. For the Microfinance Village Sample, where GPS data are available, we construct a weighted graph where the ij entry is the geographic distance between the two households.

The *union* layer has a link present if a link exists in any layer. The *intersection* layer has a link present if it exists in all layers.[6]

We also build a weighted and directed network whose edge weights are simply the sums of indicators for links in all directed layers (thus excluding jati and geography); we call this the *total* network. Finally, below we describe another weighted and directed aggregate network that we build from the principal component analysis.

2.2.1. *Descriptive Statistics.* Our first look at the data focuses on basic descriptive statistics, presented in Table 1. The different layers exhibit significantly different patterns of connection. For example, in both datasets, the social layer is denser than the other layers and has among the highest levels of clustering. We observe a higher variance of node degrees in the decision layer than in other comparable layers (e.g., advice).[7]

[5]One can also define directed networks from our data, which we comment on at several points below. Directed links open some important but tangential questions for multiplexing, which we leave for further research.

[6]Both of these definitions include the jati layer but exclude geography, since we are able to define the geographic layer for only one of our datasets, and it is a weighted network in any case. We make these definitions to maintain consistency of the meaning of the union and intersection layers across the two data sets.

[7]In the RCT villages the social layer is significantly denser than kerorice, advice, or decision layers (p-values 0.009, 0.000, and 0.000 respectively). The advice layer has significantly less variance (p-value 0.0006) and more clustering (p-value 0.03) than the decision layer. Similar patterns hold in the Microfinance villages.

TABLE 1. Descriptive Statistics

Network	degree	degree S.D.	density	triangles	clustering
Microfinance villages					
social	15.296	7.841	0.079	2635.040	0.252
kerorice	7.029	3.834	0.037	594.160	0.259
advice	6.158	3.835	0.032	299.120	0.168
decision	6.553	4.309	0.034	356.040	0.169
money	8.512	5.036	0.044	681.960	0.193
temple	1.709	1.899	0.009	52.040	0.175
medic	6.530	3.911	0.034	369.400	0.188
union link	75.428	32.542	0.368	314121.027	0.862
intersect link	0.576	0.883	0.003	7.000	0.203
jati	68.291	34.293	0.332	310150.907	1.000
RCT villages					
social	5.711	3.626	0.031	251.271	0.185
kerorice	4.910	3.235	0.027	176.557	0.174
advice	4.197	3.091	0.023	124.100	0.161
decision	4.206	3.675	0.023	125.571	0.145
union link	55.756	27.861	0.296	150771.400	0.913
intersect link	1.812	1.829	0.010	38.871	0.229
jati	52.633	28.599	0.279	150117.500	1.000

We also observe that the microfinance villages and RCT villages differ from each other in some descriptive statistics. Microfinance villages across all network layers are denser on average and exhibit higher levels of clustering, as can be seen in Table 1.[8]

Additionally, the jati layer has by far the highest degree. This finding foreshadows that jati match serves as a poor proxy for other types of relationships, being too dense, too clustered, and too homophilous to predict the other layers.

2.2.2. *Correlations among Layers.* Next, we examine the correlation among layers, pictured in Figure 1.

Figure 1 reveals several patterns. First, there are consistently high correlations between layers in both data sets—above 0.5 for most layer pairs. Second, the exceptions

[8]The two samples also differ in terms of village size. RCT villages have 197 households on average, while microfinance villages are larger with 216 households on average.

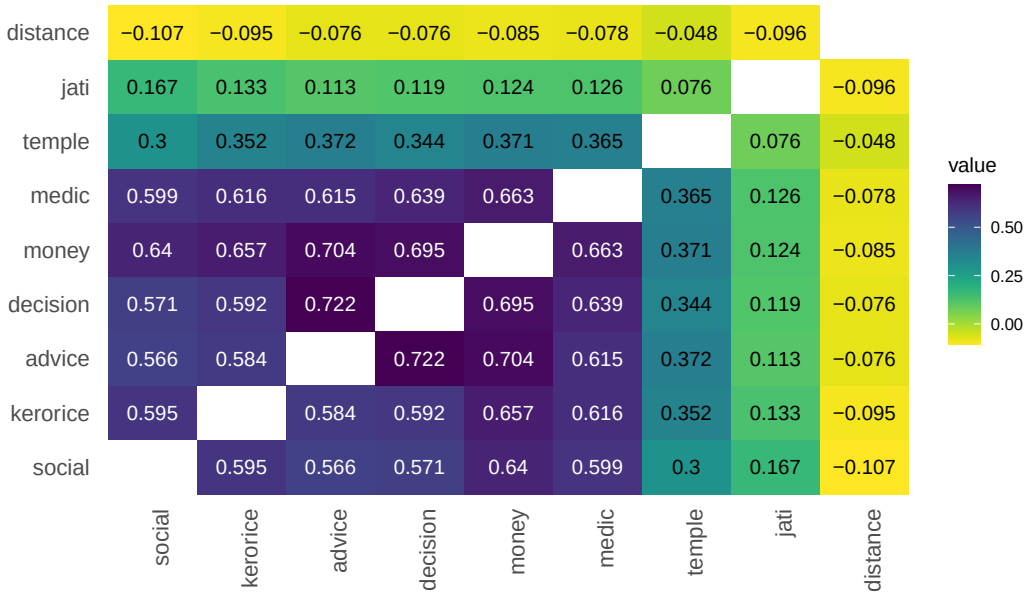

(A) Microfinance Villages

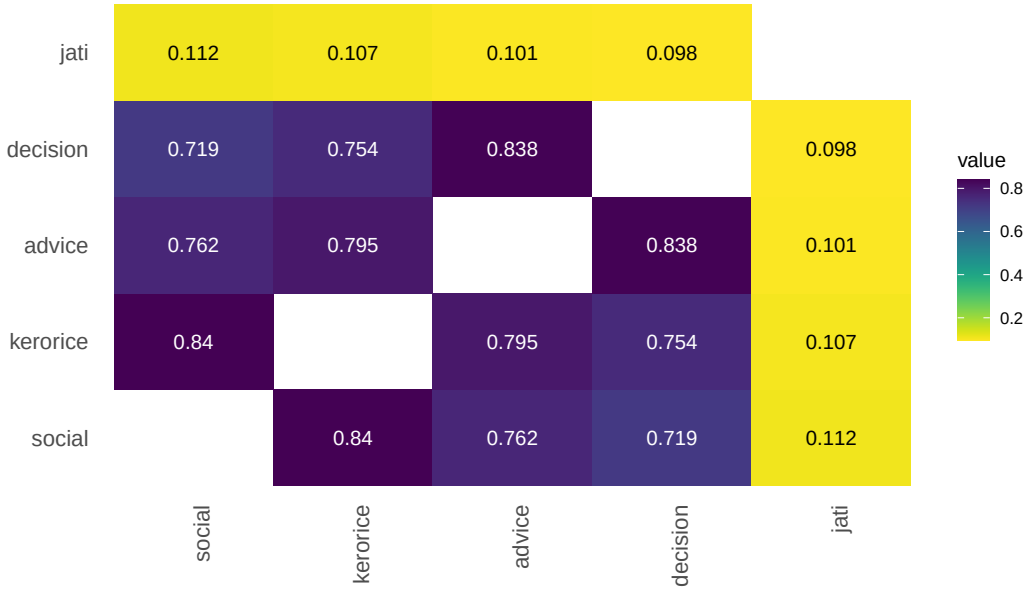

(B) RCT Villages

FIGURE 1. Correlation Heatmaps

are the distance, jati, and temple layers. The jati and distance layers are almost uncorrelated with the other layers,[9,10] while the temple layer has an intermediate level of

[9]This does not mean, for instance, that there is not substantial jati-based homophily in these data. The low correlation comes from the fact that the jati layer dramatically over-predicts relationships compared to other layers, so it has many 1's where there are 0's in the other layers.

correlation with others. Third, the layers are more highly correlated in the RCT villages compared to the microfinance villages.

2.2.3. *Principal Component Analyses.* Our third look at the structure of the networks uses principal component analyses, conducted in two stages.

First, we perform a principal component analysis with all of the layers (excluding the synthetic *union* and *intersection* layers). We treat each pair of households (in a given village) as an observation, yielding $\sum_v \binom{n_v}{2}$ observations, where n_v is the number of households in village v, and the number of dimensions is the number of layers L in the given sample.

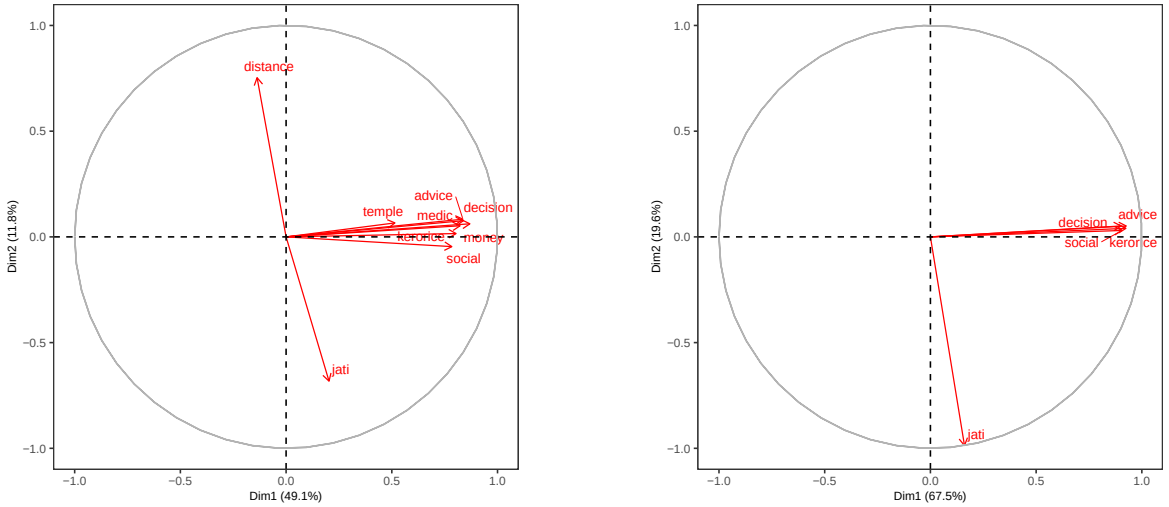

(A) Principal Components: Microfinance Villages

(B) Principal Components: Diffusion RCT

FIGURE 2. Principal Component Analysis with All Layers

As we see in Figure 2, when including all layers, the first principal component aligns with most relationship layers, capturing almost half (48.7%) of the variation in the microfinance villages and more than two-thirds (72.1%) in the RCT villages. Panels A and B plot the coordinates of the first and second component entries for each link type. Interestingly, jati largely aligns with the second principal component, as one would expect given its relatively low correlation with the other layers. The geographic distance layer is nearly opposite to jati, which reflects the fact that people from the same jati live in close proximity. The complete results appear in Appendix Tables S2 and S3.

[10]Distance is higher when people live far from each other and are thus less likely to be linked, all else held equal; this explains the negative signs.

Next, in Figure 3 we repeat the analysis after removing the least correlated dimensions: jati, geography, and temple.[11] This allows us to zoom in on the correlation patterns among the social and economic layers.

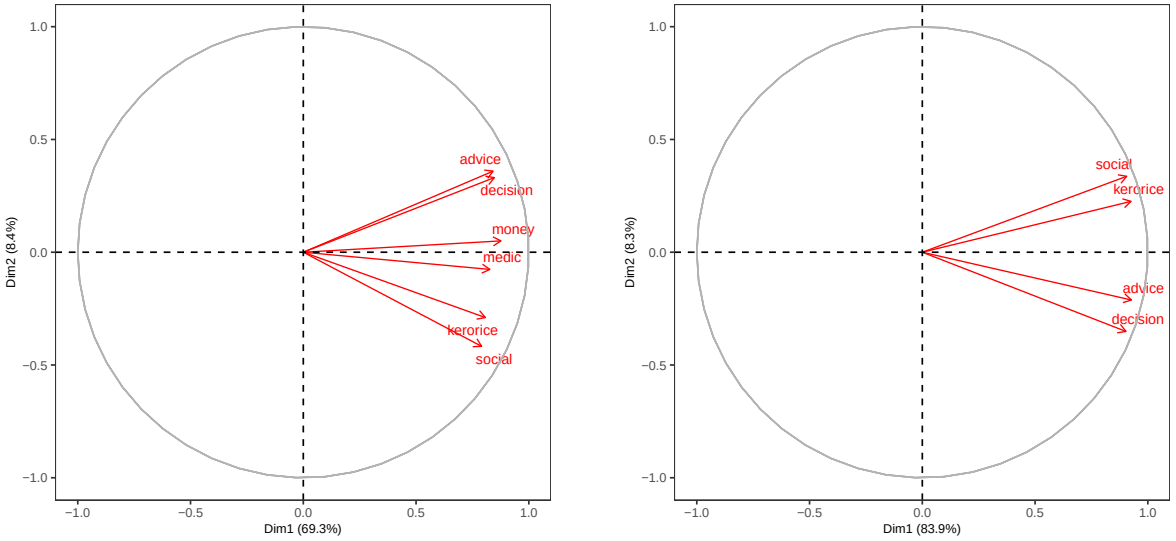

(A) Principal Components: Microfinance Villages

(B) Principal Components: Diffusion RCT

FIGURE 3. Principal Component Analysis Excluding Jati, Geography, and Temple

Figure 3 displays the relationship between the layers where we again project them on the first two principal components. In Panel A, we can see three distinct pairings of very similar layers in the microfinance villages (advice-decision, money-medic, and kerorice-social). In Panel B, there appear to be two distinct pairings in the RCT villages (advice-decision, kerorice-social), with the first component now explaining 70% and 83% of the variance across the two samples, respectively.

Building the Backbone. To capture the correlation structure of the network layers, we use the principal component analysis to construct an aggregate network from the multigraph, which we call the *backbone*. The backbone network is built using the first K principal components, constructed as described above. The K we use is determined by a so-called ladle plot, with the goal of selecting a cutoff yielding an "optimal" low-dimensional representation (see Luo and Li (2016) for details).[12]

[11] We also redo the analysis just dropping jati and geography and keeping temple in Supplemental Appendix Figure S2. Temple is sparse and essentially orthogonal to the other dimensions.

[12] To select the optimal number of principal components the literature usually relied on a cutoff based on patterns of either decreasing eigenvalues or increasing variability of eigenvectors. Luo and Li (2016) combine these two approaches to better estimate the optimal K. They propose a new estimator, called

For a pair ij in village v, we compute the weighted sum of its projections on the first K principal components as

$$Z_{ij,v} = \sum_{k=1}^{K} w_k \cdot \left(\sum_{\ell=1}^{L} g_{ij,v}^{\ell} \cdot e_{k\ell} \right).$$

In this formula, e_k is the eigenvector associated with the k^{th} principal component, and the weights w_k are determined by the relative magnitudes of the eigenvalues associated with each component:

$$w_k := \lambda_k / \sum_{j=1}^{K} \lambda_j.$$

For each village v, we then define a "backbone" network, $g^{backbone}$, from the principal components as a weighted graph where

$$g_{ij,v}^{\text{backbone}} = Z_{ij,v}.$$

In words, the backbone reduces the multiplex data to a stripped-down structure by projecting the multidimensional links onto the top principal components. After determining the number of components K, we compute each dyad's coordinates along these components, scaling by eigenvalues, which (as is standard in PCA) quantify the importance of various dimensions. Summing these weighted projections yields a single index.

2.3. **Determinants of Diffusion.**

The empirical analysis demonstrates that multiplexed networks in our data are rich and embed important information that would be lost by collapsing them into a single summary measure. A natural next question is how this distinction between layers matters for outcomes of interest. Here we focus on diffusion in the RCT villages.

We proceed as follows. Based on prior work, we would expect that more central seeds should lead to greater diffusion (Banerjee et al., 2013, 2019). Those papers defined a single network by using the union network and computed diffusion centrality based on that. However, given our rich multiplex data, we note that the seeds' diffusion centrality differs across layers. Thus, we examine which layer is the most predictive of diffusion in the RCT if we were to compute diffusion centrality based on that layer alone.

We use a specific diffusion centrality measure developed in Banerjee et al. (2013) and further studied in Banerjee et al. (2019). In particular, the *diffusion centrality* of a node

the "ladle estimator" which minimizes an objective function that incorporates both the magnitude of eigenvalues and the bootstrap variability of eigenvectors. This approach exploits the pattern that when eigenvalues are close together, their corresponding eigenvectors tend to vary greatly, and when eigenvalues are far apart, the eigenvector variability tends to be small. By leveraging both sources of information, the ladle estimator can more precisely determine the rank of the matrix, and thus the optimal number of components to retain.

j in layer ℓ in village v, $DC^{\ell}_{j,v}$ is defined by

$$DC^{\ell}_{j,v} := \left[\sum_{t}^{T}(qg^{\ell}_{v})^{t} \cdot 1\right]_{j},$$

where T is the number of rounds of communication and q is the probability of transmission in each period across any given link. Following Banerjee et al. (2019), for village v and network layer ℓ, we set $T = \text{diameter}(g^{\ell}_{v})$, and $q = 1/\lambda^{\ell}_{v}$, where λ^{ℓ}_{v} is the largest eigenvalue associated with g^{ℓ}_{v}.[13] We calculate the diffusion centrality of the seed set of village v, S_v, for layer ℓ by

$$DC^{\ell}_{v} := \sum_{j \in S_v} DC^{\ell}_{j,v}.$$

We then can calculate how diffusion varies with the diffusion centrality of the randomly assigned seed set under layer ℓ by regressing

$$y_v = \alpha^{\ell} + \beta^{\ell} \cdot DC^{\ell}_{v} + X_v\Gamma^{\ell} + \epsilon_{v,\ell} \tag{2.1}$$

where y_v represents the number of calls received from village v (a measure of diffusion of information), and X_v includes controls for number of households, its second and third powers, and number of seeds assigned in that village. We standardize all the regressors.

Table 2 depicts how differently the layers predict diffusion based on our specification in (2.1). (Supplementary Appendix Figure S1 plots the 90% and 95% confidence intervals.)

The advice layer stands out as the most predictive, and we see that the kerorice and social layers are also significantly predictive. Notably, consistent with what we observed in the correlations and principal component analysis, jati explains the least of the variation and is not significant.

Interestingly, the four synthetic networks we have mentioned that aggregate the layers in specific ways—*union, intersection, total*, and *backbone*—all perform worse than the individual layers with the exception of jati. However, this appears to be rooted in the inclusion of jati in those aggregates. In Supplement A.2 we recreate Table 2 with aggregate layers that omit jati in their construction (this applies only to *union*, *intersection*, and *backbone*). This improves their performance, with the backbone network now yielding an R^2 second only to the advice layer.

Given how correlated the layers are, we also perform a LASSO (ℓ_1-penalized) regression to select a sparse set of relevant variables that explain diffusion. We then use post-LASSO least squares to estimate how seed set centrality under the selected layer(s) affects diffusion.

[13] See Banerjee et al. (2019) for a theoretical foundation for using these as default settings in diffusion centrality.

TABLE 2. Seed Set Diffusion Centrality

	No. Calls Received								
	1	2	3	4	5	6	7	8	9
Social	4.266								
	(1.820)								
	[0.022]								
Kero/Rice		5.466							
		(2.326)							
		[0.022]							
Advice			6.410						
			(2.416)						
			[0.010]						
Decision				3.137					
				(2.226)					
				[0.164]					
Jati					1.161				
					(1.559)				
					[0.459]				
Union						1.110			
						(1.752)			
						[0.529]			
Intersection							2.220		
							(2.200)		
							[0.317]		
Backbone								1.752	
								(2.123)	
								[0.412]	
Total Links									2.158
									(1.453)
									[0.143]
Num.Obs.	68	68	68	68	68	68	68	68	68
R2	0.194	0.254	0.313	0.161	0.110	0.110	0.139	0.119	0.131
Dep Var mean	8.691	8.691	8.691	8.691	8.691	8.691	8.691	8.691	8.691

Note: Robust standard errors are given in parentheses and p-values in square brackets. Controls added: number of households, its powers, and a dummy for number of seeds in the village. Exogenous variables are the sum of Diffusion Centrality for seeds in each village for the layer. Exogenous variables have been standardized. The total links network is the raw sum of all directed network layers (excluding jati network).

The regression of interest is given by

$$y_v = \alpha + \sum_{\ell} \beta^{\ell} \cdot DC_v^{\ell} + X_v \Gamma^{\ell} + \epsilon_{v,\ell} \tag{2.2}$$

where the variables are as described in (2.1) and instead of running a separate regression for each layer, we now include all the layer variables simultaneously. We are interested in which β^{ℓ} are estimated to be non-zero and the consistent estimates of these parameters.

A complication we face here is that in order to be consistent, LASSO requires a condition called irrepresentability, which requires the regressors of interest not to be excessively correlated (Zhao and Yu, 2006). In our setting, this requirement fails since the network layers are highly correlated. To overcome this problem, we use the Puffer transformation developed by Rohe (2015) and Jia et al. (2015), which recovers irrepresentability when the number of observations exceeds the number of variables. Although

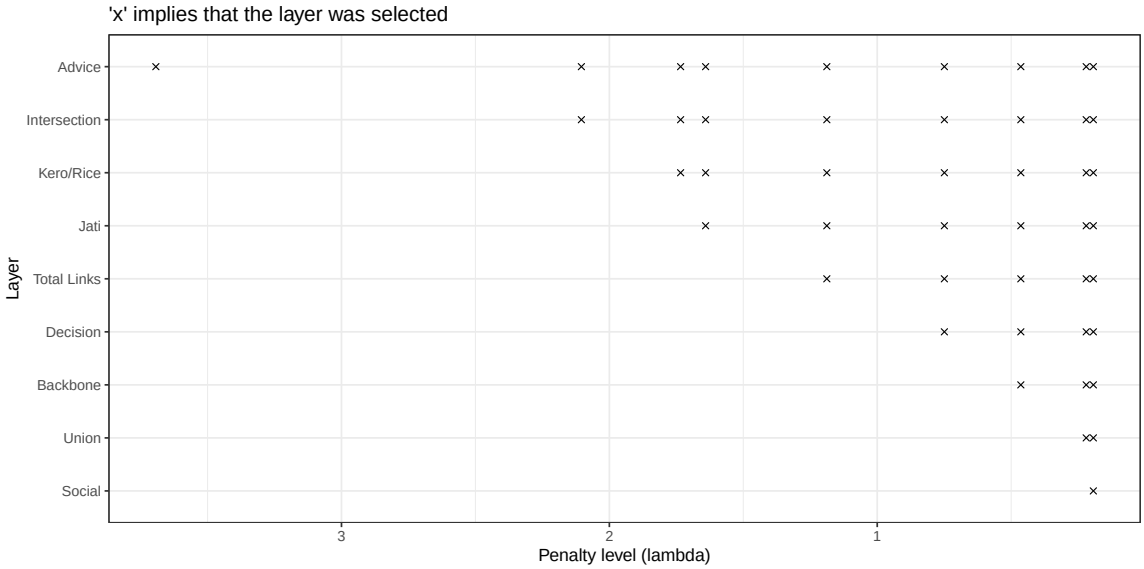

FIGURE 4. Lasso Selection of Layers in Predicting Diffusion

the regressors $(DC_v^\ell)_{v,\ell}$ have correlated columns, by appropriately pre-conditioning the data matrix, we can force its columns to be orthogonal and therefore irrepresentable. Puffer-LASSO then recovers the set of relevant variables with probability tending to one exponentially fast in the number of observations, with consistent parameter estimates, that are asymptotically normally distributed with probability approaching one (Javanmard and Montanari, 2013; Jia et al., 2015; Taylor and Tibshirani, 2015; Lee et al., 2016; Banerjee et al., 2024a).

We see the results in Figure 4, where we plot which layers are selected by the LASSO as we increase the penalty level, forcing LASSO to select fewer and fewer variables. We find that, at the highest penalty level, only the advice network layer is selected, with the post-puffer LASSO OLS regression in Table 3 depicting a 64% increase in diffusion relative to the mean ($p = 0.011$). Despite the fact that multiple layers are useful in explaining diffusion, neither the backbone, the union, nor the intersection network proved to be the most useful.

The fact that centrality in the advice layer is singled out as the best predictor of diffusion under sufficiently high penalty does not mean that the other layers have no impact on diffusion. In fact, a combination of the layers still provides significantly more prediction than just the advice layer, as shown in Table 4.

TABLE 3. Post Puffer Lasso OLS: Seed Set Diffusion Centrality

	No. Calls Received
Advice	5.564
	(2.117)
	[0.011]
Num.Obs.	68
R2	0.233
Dep Var mean	8.691

TABLE 4. F-test for the layers

layer	df	R.sq.	F-stat	p-val	F-stat marginal	p-val marginal
Advice	1	0.233	20.057	0.000		
Intersection	2	0.276	3.888	0.053	3.888	0.053
Kero/Rice	3	0.281	2.134	0.127	0.415	0.522
Jati	4	0.325	2.844	0.045	4.059	0.048
Total Links	5	0.343	2.602	0.044	1.771	0.188
Decision	6	0.348	2.159	0.070	0.478	0.492
Backbone	7	0.353	1.851	0.104	0.416	0.521
Union	8	0.353	1.564	0.164	0.021	0.884
Social	9	0.353	1.349	0.238	0.026	0.873

Table 4 presents both cumulative and marginal F-tests as variables are added in the order selected by LASSO. We can see that adding intersection is marginally significant above advice, and further including kerorice and jati yields a more complete model, with an improvement significant at the 5 percent level.[14] Thus, even though jati serves as a poor substitute for other layers, it turns out to be a useful complement to them in predicting diffusion.

2.4. **How the Level of Multiplexing Affects Diffusion.**

Next, we examine how diffusion depends on the extent to which the layers in a village are multiplexed. Specifically, do villages with greater correlation among their network layers experience higher or lower levels of diffusion? To do this, we first develop a measure of the extent to which a village is multiplexed.

[14]In Appendix Table S4 we exclude the extra layers of intersection, union, and backbone, which are "constructed" layers that are derived from these basic layers. F-tests include the basic layers in the order selected by the Lasso.

We begin by defining a multiplexing score for household i in village v as

$$m_{i,v} := \frac{\sum_j \left(\sum_\ell g^\ell_{ij,v}/L\right)}{\sum_j \mathbf{1}\{\sum_\ell g^\ell_{ij,v} > 0\}}.$$

The multiplexing score for a household i measures the average fraction of relationship types it has with each of its neighbors. The numerator calculates the average number of links household i has to each neighbor across all L relationship types. It does this by first summing the number of links between household i and each neighbor j across all layers, dividing by the total number of layers L, and then summing this average across all neighbors j. The denominator counts the number of unique neighbors of household i by summing an indicator for whether there is at least one link between i and j across any layer. For example, $m_{i,v} = 1$ if whenever household i has a relationship with some other household j, then it has all possible relationships with that other household. In contrast, when there is no multiplexing, this measure would be $1/L$.

We aggregate this to the village level by taking $m_v := \frac{1}{n_v}\sum_i m_{i,v}$. Further, we define a dummy variable for having an above-median amount of multiplexing in the sample as

$$\text{High Mpx}_v := \mathbf{1}\left\{m_v > \text{median}(m_{1:v})\right\}.$$

Our regression of interest is

$$y_v = \alpha + \beta \cdot DC_v^{advice} \times \text{High Mpx}_v + \zeta \cdot DC_v^{advice} + \eta \cdot \text{High Mpx}_v + X_v\Gamma + \epsilon_v. \tag{2.3}$$

where DC_v^{advice} denotes the diffusion centrality of the seed set in village v for the "advice" layer (which was singled out as the best predictor of diffusion).

Here, ζ captures the returns to increasing the diffusion centrality of the seed set. Since information is seeded in all networks, η captures how the extent of diffusion changes with the worst possible seeding (the theoretical intercept). The coefficient β captures how incrementally improving seeding differentially affects the extent of diffusion as a function of multiplexing.

The interaction term $DC_v^{advice} \times \text{High Mpx}_v$ is particularly important, and its coefficient of primary interest, since villages with low seed set centrality experience very little diffusion, and hence multiplexing has a very limited opportunity to make any difference in diffusion. Thus, multiplexing's marginal impact (positive or negative) should be most pronounced in settings where the seed set centrality is high.

TABLE 5. Multiplexing and Diffusion

	Calls per Household
	(1)
High Multiplexing	−0.023
	(0.016)
	[0.164]
Seed Set Centrality	0.052
	(0.016)
	[0.002]
High Multiplexing X Seed Set Centrality	−0.039
	(0.017)
	[0.022]
Num.Obs.	68

Robust standard errors are given in parentheses, while p-values are given in square brackets. Seed Set Centrality comes from the "advice" layer and has been standardized. Controls for number of seeds and average total degree across network layers have been added.

Table 5 reports the coefficient estimates. As expected, the coefficient on seed set centrality is positive and significant. We also find that both $\beta < 0$ and $\eta < 0$. Qualitatively, $\eta < 0$ indicates that more multiplexed networks generate less diffusion, with the caveat that these villages could be different for other reasons, and the coefficient is not significant. Importantly, the coefficient $\beta < 0$ indicates that villages with more central seeding—and thus higher levels of diffusion—have their diffusion impeded by multiplexing.

3. A Theory of Diffusion and Multiplexing

We now develop a theory that helps us understand how and why multiplexing affects diffusion. The stylized facts that motivate and structure this theory, established above, are: (i) the network layers are distinct but significantly correlated/multiplexed; (ii) they are differently predictive of diffusion; (iii) multiple layers are predictive of diffusion; and (iv) more multiplexed villages experience less informational diffusion.

We approach the problem at two levels. At the individual level, we examine how a node's probability of becoming infected depends on its multiplexing (for any given probability of infection among neighbors). At the population level, we aggregate the individual effects to analyze broader contagion outcomes. For this population-level analysis, we use the results about individuals as a key lemma in analyzing a canonical SIS contagion process.

Our analysis concerns two rather different types of processes within a common framework. The first is "simple" diffusion/contagion, in which a single contact is sufficient for an individual to become infected. The second is "complex" diffusion, defined as a process in which multiple contacts are needed. We analyze each type in turn, beginning

with a result about individual infection probabilities and then aggregating to the societal level.

We begin by outlining our general model of multiplexed diffusion.

3.1. **A Model of Diffusion with Multiplexing.**

We study diffusion/contagion in a society consisting of a finite set of individuals $N = \{1, \ldots, n\}$. Each individual has relationships captured via layers $\{1, \ldots, L\}$, with a generic layer represented by ℓ. In each layer ℓ, the interactions between individuals are described by a (possibly directed) network with adjacency matrix $g^\ell \in \{0,1\}^{n \times n}$, such that $g^\ell_{ij} = 1$ if there is a link from i to j in layer ℓ (interpreted as being capable of being infected by j, e.g., via i paying attention to j in a model of information flow), and 0 otherwise. We denote the multigraph consisting of L layers by $g = (g^1, g^2, \ldots, g^L)$.

Let $\mathcal{L}_{ij} = \{\ell \mid g^\ell_{ij} = 1\}$ denote the set of layers in which there is a directed link from i to j. The set of all neighbors for a given node i is denoted $\mathcal{N}_i = \{j \mid \mathcal{L}_{ij} \neq \emptyset\}$.

To track infection across time, we index discrete periods by $t \in \{0, 1, 2, \ldots\}$. At each point in time, an individual in the network is in one of two states: Susceptible (S) or Infected (I). The status of individual i at time t is denoted by the random variable $x_i(t)$. If $x_i(t) = 1$, individual i is infected at time t; if $x_i(t) = 0$, individual i is susceptible at time t. The state of the society at time t is given by the vector $x(t) = (x_1(t), x_2(t), \ldots, x_n(t)) \in \{0,1\}^n$.

At each time t, an individual's state can change based on the infection status of its neighbors. A susceptible individual i becomes infected if it receives at least τ infection transmissions from its infected neighbors in a given time period. An infected individual recovers (and becomes susceptible again) randomly with a probability δ at the end of a period. If $\tau = 1$, this represents a standard (simple) contagion process, while with a threshold $\tau > 1$ this is known as a complex contagion (Granovetter, 1978; Centola, 2010).[15]

To complete the description of the model, we examine the mechanics of contagion in more detail. Given that individuals may be connected via multiple layers, we need to define how transmission occurs through multiple layers. Let $x_{ij}(t)$ represent the (random) number of infection transmissions at time t to a susceptible node i from an infected node j, conditional on j actually being infected.[16] At most one transmission can take place per layer. We denote the distribution of infection transmissions from node j

[15]This is closely related to games on networks (Morris, 2000; Jackson and Zenou, 2014).

[16]This is related to the standard modeling of dosed exposures in the literature on contagion; see Dodds and Watts (2004).

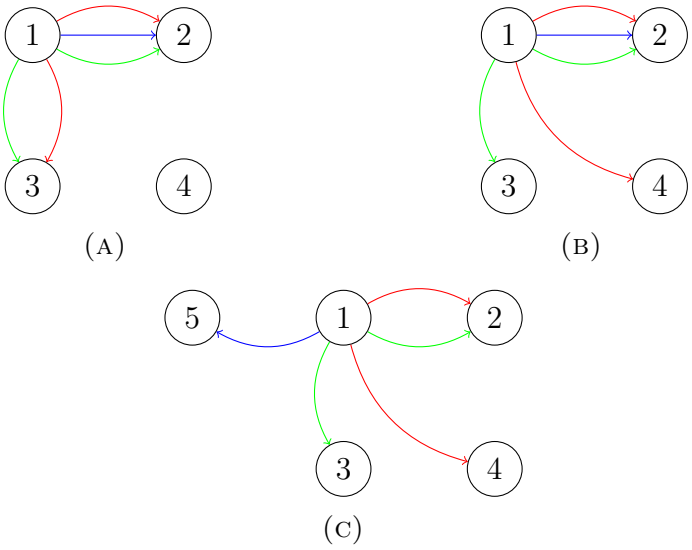

FIGURE 5. Node 1's relationships are successively less multiplexed moving from panel (A) to (C)

given $\mathcal{L}_{ij}$ by

$$f(k; \mathcal{L}_{ij}) := P(x_{ij} = k \mid \mathcal{L}_{ij}).$$

This is the probability of k transmissions; note $f(k; \mathcal{L}_{ij})$ can capture arbitrary patterns of correlation in infection transmission through multiple layers. For each layer ℓ, let $q_\ell \in (0, 1)$ be the marginal probability of infection transmission from an infected individual to a susceptible one if they are connected via that layer. We allow different layers to have different contact probabilities, which is needed given the heterogeneity in the roles of different layers discussed in Section 2.3. If there is a positive correlation in transmission across layers, two nodes connected by layers $\{A, B\}$ have an infection distribution satisfying $f(2, \{A, B\}) \geq q_A q_B$.

The probability that a susceptible individual i becomes infected at time t given the infection status of its neighbors at time $t - 1$ is

$$P\left(\sum_{j \in \mathcal{N}_i} x_{ij} x_j(t-1) \geq \tau\right)$$

3.1.1. *Comparisons of Multiplexing.* Since it is not always possible to order two multigraphs in terms of multiplexing, we define a partial order on the set of multigraphs. We begin with an example illustrating the concept in Figure 5.

In Figure 5(A) we depict a multigraph with 5 nodes and 3 layers. In Figure 5(B), by moving node 1's link in layer *red* from node 3 to node 4, we arrive at a graph that

is less multiplexed while maintaining the same out-degree. Similarly, in panel C, we again move node 1's link in layer *blue* from node 2 to node 5, creating a less multiplexed network as compared to panel B.

To formalize this type of ranking, we define a *local multiplexity dominance relation*, denoted by $\prec$. For two multigraphs g and $\widehat{g}$, we say $\widehat{g} \prec g$—that is $\widehat{g}$ is locally less multiplexed than g—if $\widehat{g}$ can be obtained from g by removing a link in some layer ℓ between nodes i and j and adding a new link in that same layer to another neighbor k, where i's connections to k occurred in a set of layers that form a strict *subset* of the layers (except layer ℓ) in which i was connected with j to start with. This means that: (i) $\mathcal{L}_{ik}(g) \subsetneq \mathcal{L}_{ij}(g) \setminus \{\ell\}$, (ii) $g^{\ell}_{ik} = 0 = \widehat{g}^{\ell}_{ij}$ and $\widehat{g}^{\ell}_{ik} = 1 = g^{\ell}_{ij}$, and (iii) for all other links $\widehat{g}$ and g coincide.

Given that the *local multiplexity dominance relation* is acyclic (see Proposition 5 in the appendix), we define the *less multiplexed relation*, denoted by $\overline{\prec}$ as the transitive closure of $\prec$. That is, we say that $\widehat{g}\overline{\prec}g$ if there exists a finite sequence of multigraphs $g_1, g_2, \ldots, g_k$ such that $\widehat{g} = g_1 \prec \cdots \prec g_k = g$. The relation $\overline{\prec}$ forms a partial order on the set of multigraphs.

We now define a corresponding notion for a particular node i. We say that $\widehat{g}\overline{\prec}_i g$ if $\widehat{g}$ is less multiplexed than g (i.e., $\widehat{g}\overline{\prec}g$) and, moreover, the changes in the network's multiplexity structure involve node i. Formally, $\widehat{g}\overline{\prec}_i g$ holds if $\widehat{g}\overline{\prec}g$ and $\widehat{g}_i \neq g_i$, where g_i denotes the collection of all layers' adjacency for node i. We refer to this refined notion as *local multiplexity dominance for node i*.

3.2. **Multiplexing Impedes Simple Diffusion and Contagion.**

We first analyze the case of simple contagion, $\tau = 1$. We focus on the case of two layers as this captures all of the essential intuition.

3.2.1. *Infection of an Individual.*

To understand how increasing multiplexing impedes diffusion, it helps to first isolate the comparison on a single pair of links while holding everything else fixed. Specifically, consider some node i that is connected in both layers A, B to node j in g, but not to another node k. Changing from g to $\widehat{g}$ involves removing one of the layers of connection from j and adding it to k. Since all other connections of i remain unaffected, only events involving the changed links need to be considered to assess the effect on i's infection probability.

Suppose that both j and k are independently infected with probability ρ, and similarly for any of i's other connections. The probability of i becoming infected by one of these

two nodes is higher from two un-multiplexed links if and only if

$$q_A\rho + q_B\rho - f(2,\{A,B\})\rho \;\;\leq\;\; q_A\rho + q_B\rho - q_Aq_B\rho^2,$$

where A, B are the layers. Simplifying this yields

$$q_Aq_B\rho \;\leq\; f(2,\{A,B\}). \tag{3.1}$$

A sufficient condition for the inequality is that $q_Aq_B \leq f(2,\{A,B\})$, or that transmissions are independent across layers. The basic intuition is that multiplexing reduces diversification of contacts across different individuals, which lowers the probability of encountering at least one infected neighbor. Under independence or weak correlation, breaking a multiplexed link into separate links to distinct neighbors generally improves diffusion.

If there is negative correlation across layers, this condition can be relaxed. As long as $\rho < 1$ (so that not everyone is infected), the diversification advantage is preserved even with some negative correlation in transmissions, provided that the negative correlation is not too severe.[17]

We summarize our observations in the following result.

Proposition 1. *Consider simple contagion ($\tau = 1$). If $\widehat{g} \overline{\prec}_i g$ and each of i's neighbors is infected independently with probability $\rho > 0$, and i is susceptible, then i is more likely to be infected under the less multiplexed network g than under $\widehat{g}$* if and only if *transmission is not too negatively correlated across layers (condition 3.1), with the reverse holding if condition 3.1 fails.*

3.2.2. *Multiplexing and Overall Infection in the SIS Model.*

Proposition 1 suggests that the overall infection rate in a variety of contagion processes should be higher on less multiplexed networks. However, our formal analysis so far only considers one node. We now extend our reasoning to the population level in the case of the SIS model.

To perform this analysis, we extend the mean-field techniques that are standardly used to solve the SIS model with one layer of links (e.g., see Pastor-Satorras and Vespignani (2000); Jackson (2008)), to study it under multiplexing.

[17]When negative correlation is very strong, multiplexing actually enhances simple diffusion processes: having connections in multiple layers to the same neighbor disperses the probability of transmission rather than concentrating it. In other words, strong negative correlation in transmission events across multiplexed links makes it less likely that one would receive two transmissions from the same neighbor, which effectively mimics the benefit of diversified contacts in the independent regime.

A given node i's connections are described by a vector $D_i = (D_{i1}, \ldots, D_{iK})$, where $K \leq n-1$ is the total number of neighbors of the node, and $D_{ik} \subseteq \{1, \ldots, L\}$ is the set of layers that i is connected to its kth neighbor on, where each $D_{ik} \neq \emptyset$.

Focusing again on the case of two layers, a sufficient statistic for D_i for the mean-field analysis is a triple $\hat{D}_i = (\hat{D}_{iA}, \hat{D}_{iB}, \hat{D}_{i,AB})$, which represents the number of connections that i has that are just on layer A, just on layer B, and on both layers, respectively. The distribution of $\hat{D}$ across the population is described by a function $P(\hat{D})$, which we assume to have finite support. The steady-state infection rate of nodes with connection profile $\hat{D}$ is denoted $\rho(\hat{D})$. The population infection rate is then defined by

$$\rho = \sum_{\hat{D}} P(\hat{D})\rho(\hat{D}). \tag{3.2}$$

The probability that a susceptible node with connections $\hat{D} = (\hat{D}_A, \hat{D}_B, \hat{D}_{AB}) \neq (0,0,0)$ becomes infected, in steady state, is then[18]

$$1 - (1 - \rho q_A)^{\hat{D}_A}(1 - \rho q_B)^{\hat{D}_B}(1 - \rho[q_A + q_B - f(2, \{A, B\})])^{\hat{D}_{AB}}. \tag{3.3}$$

In the mean-field analysis, the steady state equation for nodes with connections $\hat{D} = (\hat{D}_A, \hat{D}_B, \hat{D}_{AB}) \neq (0,0,0)$, as a function of the overall infection rate ρ, is the solution to

$$\rho(\hat{D})\delta = \tag{3.4}$$

$$(1 - \rho(\hat{D}))\left[1 - (1 - \rho q_A)^{\hat{D}_A}(1 - \rho q_B)^{\hat{D}_B}(1 - \rho(q_A + q_B - f(2, \{A, B\})))^{\hat{D}_{AB}}\right].$$

A steady-state is a joint solution to (3.2) and (3.4) for each $\hat{D}$ in the support of P. Note that 0 is always a solution, and for some distributions P there may also exist a positive solution. We focus on the largest positive solution, which is the one that corresponds to the behavior of large finite graphs.[19]

We extend the partial order we defined in 3.1.1 to the space of distributions as follows. We say that a distribution P' is less multiplexed that P, denoted by $P' \preceq P$, if there exists $\hat{D}$ and $\hat{D}'$ such that

- $\hat{D}'_A = \hat{D}_A + 1$,
- $\hat{D}'_B = \hat{D}_B + 1$,

[18]Here, $(1 - \rho q_A)$ is the probability that an infected layer-A-only neighbor fails to transmit infection, and similarly for $(1 - \rho q_B)$ for a layer-B-only neighbor. For neighbors connected via both layers, $(1 - \rho[q_A + q_B - f(2, \{A, B\})])$ is the probability that such a neighbor fails to transmit infection, accounting for potential correlation in transmissions across the two layers. Raising these terms to the powers $\hat{D}_A, \hat{D}_B, \hat{D}_{AB}$ accounts for all relevant neighbors. Multiplying them together gives the probability that *none* of these neighbors transmit infection through their respective sets of layers. Subtracting this product from 1 then yields the probability that at least one transmission succeeds, infecting the susceptible node.

[19]See Elliott et al. (2022) for a detailed argument in an analogous model.

- $\hat{D}'_{AB} = \hat{D}_{AB} - 1$,
- $P'(\hat{D}') + P'(\hat{D}) = P(\hat{D}') + P(\hat{D})$, and
- $P'(\hat{D}') > P(\hat{D}')$.

In other words, to move from P to P', we increase the frequency of profiles with separate links $(\hat{D}'_A, \hat{D}'_B)$ while reducing the number with multiplexed links $(\hat{D}'_{AB})$, holding total mass constant. The relation $\overline{\prec}$ is then defined as the transitive closure of this ordering.

Proposition 2. *Consider a simple contagion process ($\tau = 1$) process. Let transmission probabilities be given by f with marginal probabilities $(q^\ell)_\ell \in (0,1)^L$. Finally, fix a recovery rate $\delta \in (0,1)$ and two distributions of connections P' and P that each have positive steady-state infection rates. If $P' \overline{\prec} P$, then the positive steady-state infection rate under P' is higher than that under P* if and only if *transmission is not too negatively correlated (condition 3.1) at the positive infection rate of P.*

Proposition 2 implies that multiplexing has significant consequences, which can be beneficial or detrimental depending on whether diffusion is socially desirable (e.g., information about a beneficial program) or not (e.g., spread of a disease). Given the various factors that may lead to multiplexing, this implies that the mechanisms causing people to layer their networks have important implications for diffusion processes. This also means that networks whose layers are optimized for one purpose may be suboptimal for another.

3.3. **Multiplexing and Complex Diffusion.**

The results on simple contagion are unambiguous: multiplexing impedes simple diffusion/contagion except in extreme cases of negatively correlated transmission probabilities. Complex contagion, in contrast, presents a more nuanced picture. Multiplexing can both enhance and impede diffusion, depending on the circumstances.

In complex diffusion, two competing forces of multiplexing emerge. One force mirrors the effect seen in simple contagion: diversifying links increases the probability of at least some links reaching infected individuals. However, a counterforce now exists: conditional on reaching an infected individual, multiplexing leads to higher probabilities of multiple transmissions, compared to spreading those links across other individuals who might be uninfected. This makes it more likely that a contagion threshold greater than 1 is reached.

To keep the analysis as uncluttered as possible, we again focus on the case of two layers. We also consider a case where the correlation in transmission across layers is neither too high nor too low, so that there is an ε, to be determined in the proofs of the

propositions below, for which $(1+\varepsilon)q_Aq_B \geq f(2,\{A,B\}) \geq q_Aq_B$. Of course, a sufficient condition for this to hold is independent transmission. This condition is needed as with excessive positive or negative correlation in transmission, strange discrete behavior in transmission as a function of multiplexing can occur.[20] The assumption we are imposing allows the results to highlight the more fundamental forces of multiplexing.

Proposition 3. *Consider a complex contagion ($\tau > 1$). Fix a susceptible node i such that i's neighbors are infected independently with probability $\rho > 0$, and two networks such that $\widehat{g} \overline{\prec}_i g$. Also suppose that $\sum_{\ell,j} g^{\ell}_{ij} > \tau$, so that i has more than enough connections to become infected.*

There exist $0 < \underline{\rho} < \overline{\rho} < 1$ such that

- *if $\rho, q_A, q_B > \overline{\rho}$, then i is* less *likely to be infected under the more multiplexed network g than under $\widehat{g}$, and*
- *if $\rho, q_A, q_B < \underline{\rho}$, then i is* more *likely to be infected under the more multiplexed network g than under $\widehat{g}$.*

The intuition behind this result is as follows. There exist nodes i, j, k such that under g, node i is connected to j on two layers and to k on none, while under $\widehat{g}$, node i is connected to j on one layer and to k on the other. The cases in which this difference can be pivotal are when the other connections to other nodes have led to either $\tau - 1$ or $\tau - 2$ transmissions. With very high infection and transmission rates among neighbors, the $\tau - 1$ case predominates, making the situation resemble simple contagion—thus, less multiplexing leads to a higher chance of infection. Under very low infection rates, the $\tau - 2$ case becomes more likely, requiring two incremental infections. This is highly improbable across two separate neighbors but much more likely with a single neighbor, making more multiplexing advantageous for infection probability.

Interestingly, as we will see in the simulations below, these forces can interact non-monotonically in the intermediate range for infection and transmission rates, which explains the gap between the upper and lower bounds.

We now state how this translates into an aggregate infection rate.

Proposition 4. *Consider a complex contagion ($\tau > 1$), with nonnegative correlation in transmission across layers, so that $f(2,\{A,B\}) \geq q_Aq_B$, and two distributions such that $P' \overline{\prec} P$ and both have positive steady-state infection rates. Also suppose that $\hat{D}_A + \hat{D}_B +$*

[20] For instance, if transmission is perfectly positively correlated, then one is always more likely to get two transmissions from a single multiplexed connection than two unmultiplexed connections, but is always more likely to get one transmission from the reverse. This then implies that the optimal configuration of connections depends on whether τ is even or odd, in complicated ways as a function of a node's overall degrees in each layer.

$2\hat{D}_{AB} > \tau$ for each $\hat{D}$ in the distribution P, so that each node has more than enough connections to become infected. There exist $0 < \underline{\rho} < \overline{\rho} < 1$ such that

- *if $q_A, q_B < \underline{\rho}$ and δ is sufficiently high, then the steady-state infection is higher for P than P', and*
- *if $q_A, q_B > \overline{\rho}$ and δ is sufficiently low, then the steady-state infection is lower for P than P'.*

Note that the steady-state infection of every connection type shares the same ordering as the overall infection rate.

3.4. **Simulations.** The theoretical results are based on the asymptotic statistical behavior of large random networks. To see how the results work in smaller empirical networks, we run simulations on the networks from the RCT villages. We simulate a Susceptible-Infected-Susceptible (SIS) diffusion process for the cases of both simple and complex diffusion and compare outcomes as multiplexing is varied. In order to compare across similar-sized networks where only multiplexing is changing, we take a given village network and construct two-layer networks by combining different pairs of empirical networks (which end up empirically having different multiplexing rates), in a way we specify below. We then perform many diffusion simulations on these two-layer networks for each village.

More specifically, for each village, we begin by picking three empirical adjacency matrices representing different network layers sorted in decreasing order of their average out-degree: A_1, A_2, and A_3. We then pair A_1 with A_2 for one simulated diffusion, and A_1 with A_3 for the other. To ensure that the average out-degree is comparable across the networks, we prune at random the links in A_2 to match the average out-degree of A_3, resulting in a pruned network $A_2^{'}$. We construct two multiplexed networks: g', by combining A_1 and $A_2^{'}$, and g, by combining A_1 with the A_3. The process is presented in full detail in the Appendix (Algorithm 2).

The diffusion process (also presented in full detail in the appendix in Algorithm 1), is as follows. First, a susceptible node can get message transmissions from each infected neighbor in each layer, i.i.d., with probability q in each period. Second, a susceptible node gets infected only if it receives at least $\tau \geq 1$ contacts in a given time period and the count resets in each time period. Third, in each period an infected node transitions back to being susceptible with probability δ. We terminate the simulation when the share of infected nodes changes by less than a small threshold between consecutive iterations. In our simulations, we use $\tau = 1$ for simple diffusion and $\tau = 2$ for complex. In each simulation we set the number of randomly selected seeds in the initial period

to be $\lfloor \sqrt{n} \rfloor$, where n is the number of households in the network. For both, simple diffusion ($\tau = 1$) as well as complex diffusion ($\tau = 2$) we run simulations on a grid of $(q, \delta) \in [0.1, 0.5] \times [0.1, 0.5]$. We run the diffusion simulations 500 times for each village across both multiplexed networks g, g' described above. We report the averages across all 70 villages.

Given that these are smaller networks, some simulations end up randomly having more or less diffusion in any given run across the two comparison networks. Thus, we tabulate the fraction of simulation runs for which more multiplexing is associated with more diffusion.

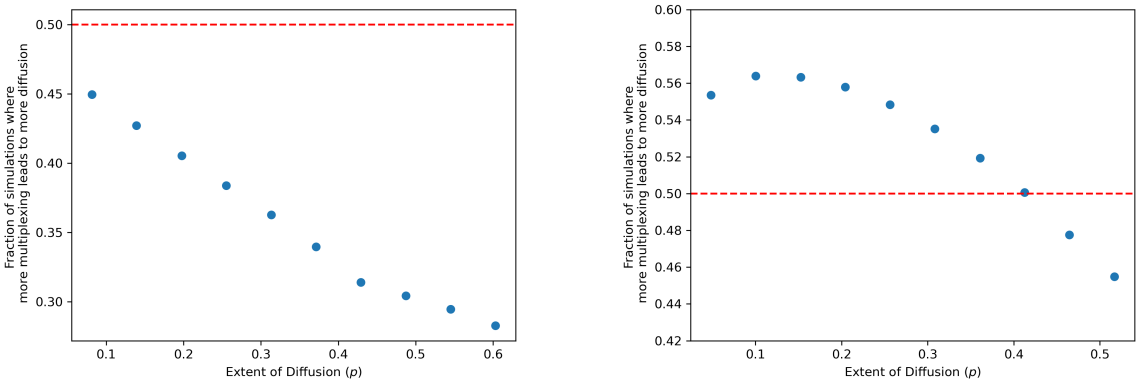

(A) Simple Contagion ($\tau = 1$) (B) Complex Contagion ($\tau = 2$)

FIGURE 6. Diffusion Simulations

In Figure 6 we plot the fraction of simulation runs where more multiplexing leads to more diffusion against the extent of diffusion in the network p. In panel A, we plot the results for simple diffusion. We find that higher multiplexing is consistently associated with lower diffusion levels, as in our theoretical results.

In panel B we see the nonmonotonicity from the countervailing forces in complex diffusion that we mentioned in Section 3.3. We also see a confirmation of the theoretical results. At low levels of diffusion, the steady state diffusion is increasing in multiplexing, and for high diffusion levels, the steady state diffusion is decreasing in multiplexing.

4. Concluding Discussion

Our study began by descriptively examining patterns of multiplexing. We next showed that multiplexing systematically impacts diffusion, via both experimental evidence and theoretical modeling.

Our findings highlight the need for future work on incentives to multiplex and the consequences of multiplexing decisions. There are several immediate directions to explore. For example, our results suggest that the deeper the need to form reinforced or supported (i.e., multiplexed) relationships, the greater the potential inefficiencies in certain domains. In particular, those who are under weaker institutions or have limited resources may face a greater need to multiplex relative to their richer counterparts. Consequently, they may experience both reduced access to information and increased susceptibility to the spread of social norms that are described by complex contagion dynamics—a susceptibility that may be beneficial or detrimental.

There is also a need for further development of measures and methods of analyzing multiplexed networks. We defined one of many potential measures of how multiplexed a network is, as well as one of many potential partial orders. Understanding which measures are most appropriate in which settings is a subject for further research.

To close, we report two other patterns that we found in the data. For both of the following calculations, we use the multiplexing score that we defined in Section 2.4:

$$m_{i,v} := \frac{\sum_j \left(\sum_\ell g^\ell_{ij,v} / L \right)}{\sum_j \mathbf{1}\{\sum_\ell g^\ell_{ij,v} > 0\}},$$

where i represents either an individual or a household, depending on the analysis.

The first pattern is that higher-degree households are less multiplexed. We restrict our attention to the elicited layers in the RCT villages: the social, kerorice, advice, and decision layers. Figure 7 depicts a binned scatter plot where we can see that households that have higher degree (aggregated across layers) have lower levels of multiplexing.

The second pattern is that women's networks are significantly more multiplexed than those of men. Here we use the microfinance villages, where we have access to individual-level network data. We focus on the social, kerorice, advice, decision, money, temple, and medic layers. For each village v, we aggregate this score at the gender level: $m_{a,v} = \frac{1}{n_a} \sum_{i \in I_a} m_{i,v}$, where $a \in \{\text{male}, \text{female}\}$. Figure 8 shows the density curves for these multiplexing scores across the villages, as well as for each individual treated as a separate observation. The distributions reveal that women's networks are systematically more multiplexed. In Supplemental Appendix Figure S3 we include the same analysis with a different wave of data, and see an even starker difference.

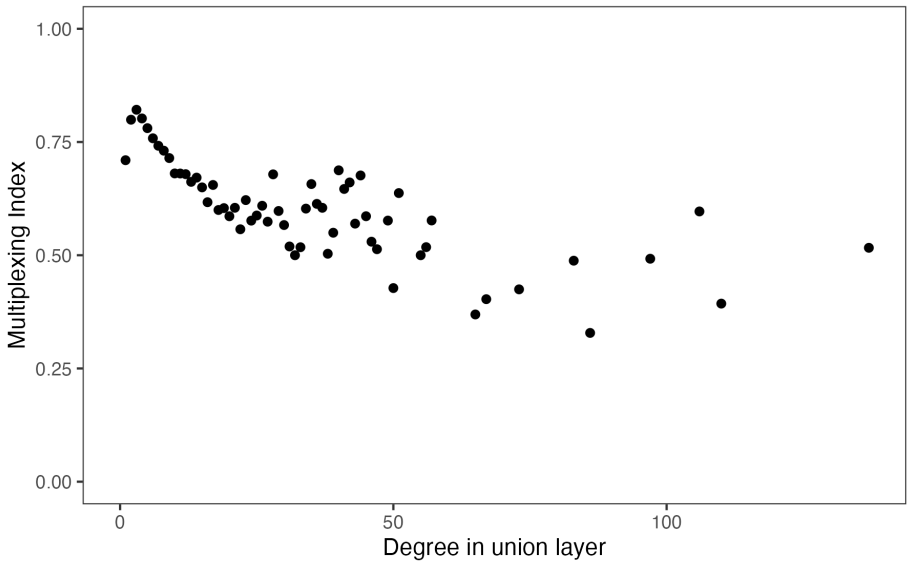

FIGURE 7. Multiplexing as a function of degree.

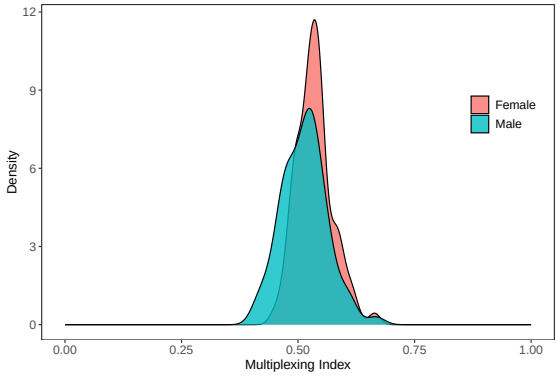

(A) Density: Aggregate

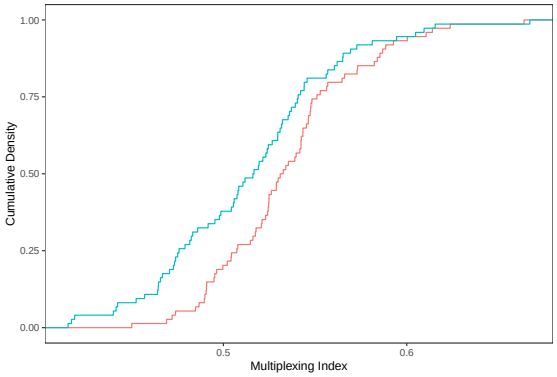

(B) Cumulative Density: Aggregate

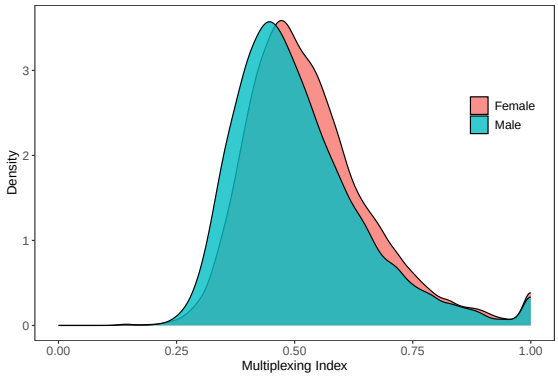

(C) Density: Individual

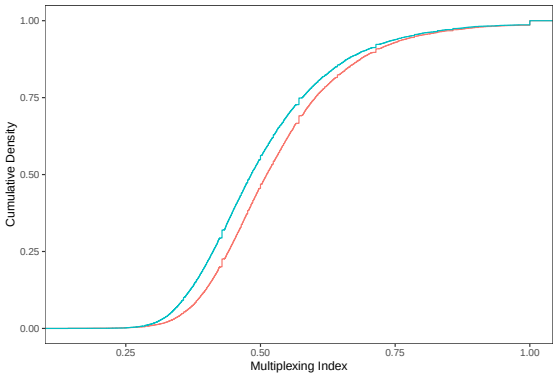

(D) Cumulative Density: Individual

FIGURE 8. Multiplexing by Gender. The aggregate plots average over a given gender within a village and then depict the distribution of the resulting numbers for that gender. The individual plots include each person as a separate observation.

This result could help explain results of Beaman and Dillon (2018), who found unexplained differences in diffusion by gender. To understand potential sources of gender differences in multiplexing, note that women in rural Indian communities often marry across village boundaries (though frequently still within the constraints of caste/jati endogamy) and most of these marriages are virilocal—requiring the wife to move into the husband's house (Rosenzweig and Stark, 1989; Rao and Finnoff, 2015). As a consequence, women often rely on affinal kin and over time need to "rebuild" their networks (Hruschka et al., 2023). This occurs in conjunction with the expectation that these women take on various responsibilities, including agricultural work, managing the household, preparing meals, and raising children. Such constraints on available relationships while serving multiple roles can plausibly result in high levels of multiplexing, an interesting subject for further research.

References

Ambrus, A., M. Mobius, and A. Szeidl (2014): "Consumption risk-sharing in social networks," *American Economic Review*, 104, 149–182. 1

Atkisson, C., P. J. Górski, M. O. Jackson, J. A. Hołyst, and R. M. D'Souza (2019): "Why understanding multiplex social network structuring processes will help us better understand the evolution of human behavior," *forthcoming: Evolutionary Anthropology*. 1

Banerjee, A., A. G. Chandrasekhar, S. Dalpath, E. Duflo, J. Floretta, M. O. Jackson, H. Kannan, F. N. Loza, A. Sankar, A. Schrimpf, et al. (2024a): "Selecting the Most Effective Nudge: Evidence from a Large-Scale Experiment on Immunization," *Econometrica, forthcoming*. 2.3

Banerjee, A., A. G. Chandrasekhar, E. Duflo, and M. O. Jackson (2019): "Using gossips to spread information: Theory and evidence from two randomized controlled trials," *The Review of Economic Studies*, 86, 2453–2490. 1, 2.1.2, 2.3, 13

Banerjee, A. V., E. Breza, A. G. Chandrasekhar, E. Duflo, M. O. Jackson, and C. Kinnan (2024b): "Changes in Social Network Structure in Response to Exposure to Formal Credit Markets," *Review of Economic Studies*, 91:3, 1331–72. 1, 2.1.1

Banerjee, A. V., A. G. Chandrasekhar, E. Duflo, and M. O. Jackson (2013): "Diffusion of Microfinance," *Science*, 341, DOI: 10.1126/science.1236498, July 26 2013. 1, 2.1.1, 2.3, A.1

Beaman, L. and A. Dillon (2018): "Diffusion of agricultural information within social networks: Evidence on gender inequalities from Mali," *Journal of Development*

Economics, 133, 147–161. 4

Becker, S. O., Y. Hsiao, S. Pfaff, and J. Rubin (2020): "Multiplex network ties and the spatial diffusion of radical innovations: Martin Luther's leadership in the early reformation," *American Sociological Review*, 85, 857–894. 1

Bianconi, G. (2018): *Multilayer networks: structure and function*, Oxford university press. 1

Billand, P., C. Bravard, S. Joshi, A. S. Mahmud, and S. Sarangi (2023): "A model of the formation of multilayer networks," *Journal of Economic Theory*, 213, 105718. 1

Boccaletti, S., G. Bianconi, R. Criado, C. I. Del Genio, J. Gómez-Gardenes, M. Romance, I. Sendina-Nadal, Z. Wang, and M. Zanin (2014): "The structure and dynamics of multilayer networks," *Physics reports*, 544, 1–122. 1

Centola, D. (2010): "The Spread of Behavior in an Online Social Network Experiment," *Science*, 329: 5996, 1194–1197, DOI: 10.1126/science.1185231. 3.1

Cheng, C., W. Huang, and Y. Xing (2021): "A theory of multiplexity: Sustaining cooperation with multiple relations," *Available at SSRN 3811181*. 1

Contractor, N., P. Monge, and P. M. Leonardi (2011): "Network Theory—multidimensional networks and the dynamics of sociomateriality: bringing technology inside the network," *International Journal of Communication*, 5, 39. 1

Dickison, M. E., M. Magnani, and L. Rossi (2016): *Multilayer social networks*, Cambridge University Press. 1

Dodds, P. S. and D. J. Watts (2004): "Universal behavior in a generalized model of contagion," *Physical review letters*, 92, 218701. 16

Elliott, M., B. Golub, and M. V. Leduc (2022): "Supply network formation and fragility," *American Economic Review*, 112, 2701–2747. 19

Fafchamps, M. and F. Gubert (2007): "Risk sharing and network formation," *American Economic Review*, 97, 75–79. 1, 2.1.1

Granovetter, M. S. (1978): "Threshold models of collective behavior," *American journal of sociology*, 83, 1420–1443. 3.1

Hruschka, D. J., S. Munira, and K. Jesmin (2023): "Starting from scratch in a patrilocal society: how women build networks after marriage in rural Bangladesh," *Philosophical Transactions of the Royal Society B*, 378, 20210432. 4

Hu, Y., D. Zhou, R. Zhang, Z. Han, C. Rozenblat, and S. Havlin (2013): "Percolation of interdependent networks with intersimilarity," *Physical Review E—Statistical, Nonlinear, and Soft Matter Physics*, 88, 052805. 1

Jackson, M. O. (2008): *Social and economic networks*, Princeton: Princeton University Press. 3.2.2

Jackson, M. O., S. M. Nei, E. Snowberg, and L. Yariv (2024): "The Dynamics of Networks and Homophily," *SSRN Working Paper https://papers.ssrn.com/abstract=4256435*, . 1

Jackson, M. O. and Y. Zenou (2014): "Games on Networks," *Handbook of Game Theory, Elsevier, edited by Young, H.P. and Zamir, S.* 15

Javanmard, A. and A. Montanari (2013): "Model selection for high-dimensional regression under the generalized irrepresentability condition," in *Proceedings of the 26th International Conference on Neural Information Processing Systems-Volume 2*, 3012–3020. 2.3

Jia, J., K. Rohe, et al. (2015): "Preconditioning the lasso for sign consistency," *Electronic Journal of Statistics*, 9, 1150–1172. 2.3

Kivela, M., A. Arenas, J. P. Gleeson, Y. Moreno, and M. A. Porter (2014): "Multilayer Networks," *arXiv:1309.7233v4 [physics.soc-ph]*. 1

Kobayashi, T. and T. Onaga (2023): "Dynamics of diffusion on monoplex and multiplex networks: A message-passing approach," *Economic Theory*, 76, 251–287. 1

Larson, J. M. and P. L. Rodriguez (2023): "The risk of aggregating networks when diffusion is tie-specific," *Applied Network Science*, 8, 21. 1

Lee, J. D., D. L. Sun, Y. Sun, and J. E. Taylor (2016): "Exact post-selection inference, with application to the lasso," *The Annals of Statistics*, 44, 907–927. 2.3

Luo, W. and B. Li (2016): "Combining eigenvalues and variation of eigenvectors for order determination," *Biometrika*, 875–887. 2.2.3, 12

Morelli, S. A., D. C. Ong, R. Makati, M. O. Jackson, and J. Zaki (2017): "Empathy and well-being correlate with centrality in different social networks," *Proceedings of the National Academy of Sciences*, 114, 9843–9847. 1

Morris, S. (2000): "Contagion," *Review of Economic Studies*, 67 (1), 57–78. 15

Munshi, K. and M. Rosenzweig (2009): "Why is Mobility in India so Low? Social Insurance, Inequality, and Growth," *mimeo*. 2.1.1

Pastor-Satorras, R. and A. Vespignani (2000): "Epidemic Spreading in Scale-Free Networks," *Physical Review Letters*, 86 (14), 3200–3203. 3.2.2

Rao, S. and K. Finnoff (2015): "Marriage migration and inequality in India, 1983–2008," *Population and Development Review*, 41, 485–505. 4

Rohe, K. (2015): "Preconditioning for classical relationships: a note relating ridge regression and OLS p-values to preconditioned sparse penalized regression," *Stat*, 4, 157–166. 2.3

Rosenzweig, M. R. and O. Stark (1989): "Consumption smoothing, migration, and marriage: Evidence from rural India," *Journal of political Economy*, 97, 905–926. 4

Sacerdote, B. (2001): "Peer effects with random assignment: Results for Dartmouth roommates," *The Quarterly journal of economics*, 116, 681–704. 2.1.1

San Román, D. (2024): "Multiplexed Network Formation and Bonacich Centrality," *Available at SSRN 4704738*. 1

Simmel, G. (1908): *Sociology: Investigations on the Forms of Sociation*, Leipzig: Duncker and Humblot. 1

Taylor, J. and R. J. Tibshirani (2015): "Statistical learning and selective inference," *Proceedings of the National Academy of Sciences*, 112, 7629–7634. 2.3

Townsend, R. M. (1994): "Risk and Insurance in Village India," *Econometrica*, 62, 539–591. 1

Walsh, A. M. (2019): "Games on multi-layer networks," . 1

Wasserman, S. and K. Faust (1994): *Social Network Analysis*, Cambridge: Cambridge University Press. 1

Yağan, O. and V. Gligor (2012): "Analysis of complex contagions in random multiplex networks," *Physical Review E—Statistical, Nonlinear, and Soft Matter Physics*, 86, 036103. 1

Zenou, Y. and J. Zhou (2024): "Games on Multiplex Networks," *Available at SSRN 4772575*. 1

Zhao, P. and B. Yu (2006): "On model selection consistency of Lasso," *The Journal of Machine Learning Research*, 7, 2541–2563. 2.3

Zhu, S.-S., X.-Z. Zhu, J.-Q. Wang, Z.-P. Zhang, and W. Wang (2019): "Social contagions on multiplex networks with heterogeneous population," *Physica A: Statistical Mechanics and its Applications*, 516, 105–113. 1

Appendix A. Proofs

Proof of Proposition 1: We adopt the notation from Proposition 2, as given independent probabilities of infection of neighbors, the probability that an individual with connection profile $\hat{D} = (\hat{D}_A, \hat{D}_B, \hat{D}_{AB})$ on network g becomes infected is then (from (3.3) given by

$$1 - (1 - \rho q_A)^{\hat{D}_A}(1 - \rho q_B)^{\hat{D}_B}(1 - \rho[(q_A + q_B - f(2, \{A, B\})])^{\hat{D}_{AB}}.$$

If the change is to network $\widehat{g}$ in which this individual is less multiplexed then their connection profile is $(\hat{D}_A + a, \hat{D}_B + a, \hat{D}_{AB} - a)$ for some integer $a > 0$, and then their probability of being infected is

$$1 - (1 - \rho q_A)^{\hat{D}_A + a}(1 - \rho q_B)^{\hat{D}_B + a}(1 - \rho[(q_A + q_B - f(2, \{A, B\})])^{\hat{D}_{AB} - a}.$$

The second probability is larger than the first if and only if

$$(1 - \rho q_A)^a (1 - \rho q_B)^a (1 - \rho[(q_A + q_B - f(2, \{A, B\})])^{-a} < 1,$$

which simplifies to

$$(1 - \rho q_A)(1 - \rho q_B) < (1 - \rho[(q_A + q_B - f(2, \{A, B\})]).$$

This holds if and only if

$$\rho q_A q_B < f(2, \{A, B\}),$$

which is the claimed condition. ∎

Proof of Proposition 2: Following the argument from the proof of Proposition 1, for any ρ equation 3.4 has a higher solution for the less multiplexed type. Thus, starting with the steady state ρ for the more multiplexed distribution, the new rates for all individuals are weakly and sometimes strictly higher for the less multiplexed distribution. This leads to a higher ρ'. Iterating, this converges upward for all types to a limit which is the steady state. Conversely, if condition 3.1 is reversed, the convergence is downward for all types. ∎

Proof of Proposition 3: It is enough to consider an individual i with one change in their links where a multiplexed link to j is then split to two neighbors j, k, each of which is connected to i on a different layer and where i was initially not connected to k. Our focus is on the pivotal cases:

(1) The number of infected messages i has already received from other neighbors is either $\tau - 1$ or $\tau - 2$. (That both of these cases can occur with positive probability uses the condition that $\sum_{\ell,j} g_{ij}^{\ell} > \tau$, so that there are at least $\tau - 1$ layer-connections from i to others besides j, k.)
(2) At least one of the neighbors j and k is infected.

The conditional probability (given that one is in one of these four cases) that i gets infected can be found in the table below. The top entry in each cell represents the multiplexing scenario and the bottom represents the unmultiplexed case.

	$\tau-1$	$\tau-2$
both j,k infected	$q_A+q_B-f(2,\{A,B\})$ $\wedge\vert$ $q_A+q_B-q_Aq_B$	$f(2,\{A,B\})$ $\vee\vert$ q_Aq_B
one of j,k infected	$(q_A+q_B-f(2,\{A,B\}))/2$ $\wedge$ $(q_A+q_B)/2$	$f(2,\{A,B\})/2$ $\vee$ 0

The inequality indicates which probability is larger. The $\tau-1$ column (aggregating over both rows which have positive probability) has strictly higher probability for the unmultiplexed case, while the $\tau-2$ column has strictly higher probability for the multiplexed case. Let ϕ be the probability on the first column and ψ on the second column, and note that the conditional probability of the first row is ρ^2 and the second row is $2\rho(1-\rho)$. The differences in overall probabilities of infection of the multiplexed minus unmultiplexed is then

$$(\psi-\phi)\left[\rho^2(f(2,\{A,B\})-q_Aq_B)+2\rho(1-\rho)f(2,\{A,B\})/2\right].$$

Given that $f(2,\{A,B\})-q_Aq_B\geq 0$, then this expression has the sign of $(\psi-\phi)$. The proof is then completed by noting that for high enough ρ,q_A,q_B the first column becomes more likely than the second, and for low enough ρ,q_A,q_B the second column becomes more likely than the first.This is where the condition that $(1+\varepsilon)q_Aq_B\geq f(2,\{A,B\})\geq q_Aq_B$ is invoked. With independent signal transmission across layers, for low enough ρ,q_A,q_B, it is strictly more probable to have fewer than more signals from the connections other than j,k, and thus $\psi-\phi>0$. These probabilities are continuous in f and so this holds for some $\varepsilon>0$. The reverse is true for high enough ρ,q_A,q_B. ∎

Proof of Proposition 4: We begin with the case of sufficiently low q_A,q_B and high δ. In that case ρ will also be low (an absolute bound is simply $(q_A+q_B)/\delta$ as that is a crude upper bound on the infection rate of any given node that always has all neighbors infected and needs only one signal). Then we can invoke Proposition 3 for each connection configuration (noting that there are a finite number of them, taking the min over the $\underline{\rho}$), and then the remaining argument is analogous to the proof of Proposition 2. The reverse holds for the case of sufficiently high q_A,q_B and low δ. ∎

Proposition 5. *The relation $\prec$ is acyclic.*

Proof of Proposition 5 Recall that we denote the set of layers a link ij belongs to by $\mathcal{L}_{ij}$. Define the total multiplexity index of a multigraph g as $S_g = \sum_{i>j} |\mathcal{L}_{ij}|^2$.

We show that if $\widehat{g} \prec g$, then $S_g > S_{\widehat{g}}$. By our definition of $\widehat{g} \prec g$, we know that there exist nodes i, j, k and layers ℓ, ℓ' such that $g^{\ell}_{ik} = 0 = \widehat{g}^{\ell}_{ij}$ and $\widehat{g}^{\ell}_{ik} = 1 = g^{\ell}_{ij}$, all else being equal. We only focus on the contribution of these edges in total multiplexing index since all other links are identical across the two multigraphs. For the multigraph g, this can be represented as $|\mathcal{L}_{ij}|^2 + |\mathcal{L}_{ik}|^2$, while for the less multiplexed graph $\widehat{g}$, the contribution of these edges can be written as $(|\mathcal{L}_{ij}| - 1)^2 + (|\mathcal{L}_{ik}| + 1)^2$. We can then write the difference in total multiplexing between g and $\widehat{g}$ as

$$\begin{aligned} S_g - S_{\widehat{g}} &= |\mathcal{L}_{ij}|^2 + |\mathcal{L}_{ik}|^2 - (|\mathcal{L}_{ij}| - 1)^2 - (|\mathcal{L}_{ik}| + 1)^2 \\ &= |\mathcal{L}_{ij}|^2 + |\mathcal{L}_{ik}|^2 - |\mathcal{L}_{ij}|^2 - |\mathcal{L}_{ik}|^2 - 2 + 2|\mathcal{L}_{ij}| - 2|\mathcal{L}_{ik}| \\ &= 2(|\mathcal{L}_{ij}| - (|\mathcal{L}_{ik}| + 1)) \end{aligned}$$

By $\widehat{g} \prec g$, we know that $|\mathcal{L}_{ik}| < |\mathcal{L}_{ij}| - 1$ (recall that we assumed i and j were linked in at least two layers), hence $S_g > S_{\widehat{g}}$

Now, assume that there exists a cycle such that we have a sequence of multigraphs g_i with $g_1 \prec g_2 \prec g_3 \prec \cdots \prec g_n \prec g_1$. But our proof implies $S_{g_1} < S_{g_2} < S_{g_3} < \cdots < S_{g_n} < S_{g_1}$, which gives us a contradiction. Hence the relation is acyclic. ∎

Supplementary Appendix:

Multiplexing in Networks and Diffusion

by Chandrasekhar, Chaudhary, Golub, Jackson

A.1. **Supplementary Figures.**

Figure S1 plots the results from Table 2. $\hat{\beta}^{\ell}$ and both the 90% and 95% confidence intervals for each of the distinct layers are plotted. Seed centrality in the jati network is not statistically significantly associated with diffusion ($p = 0.459$). Seed centrality in the advice, social, and kerorice networks all are significantly positively associated with diffusion. The point estimates are large, roughly a 59% increase.

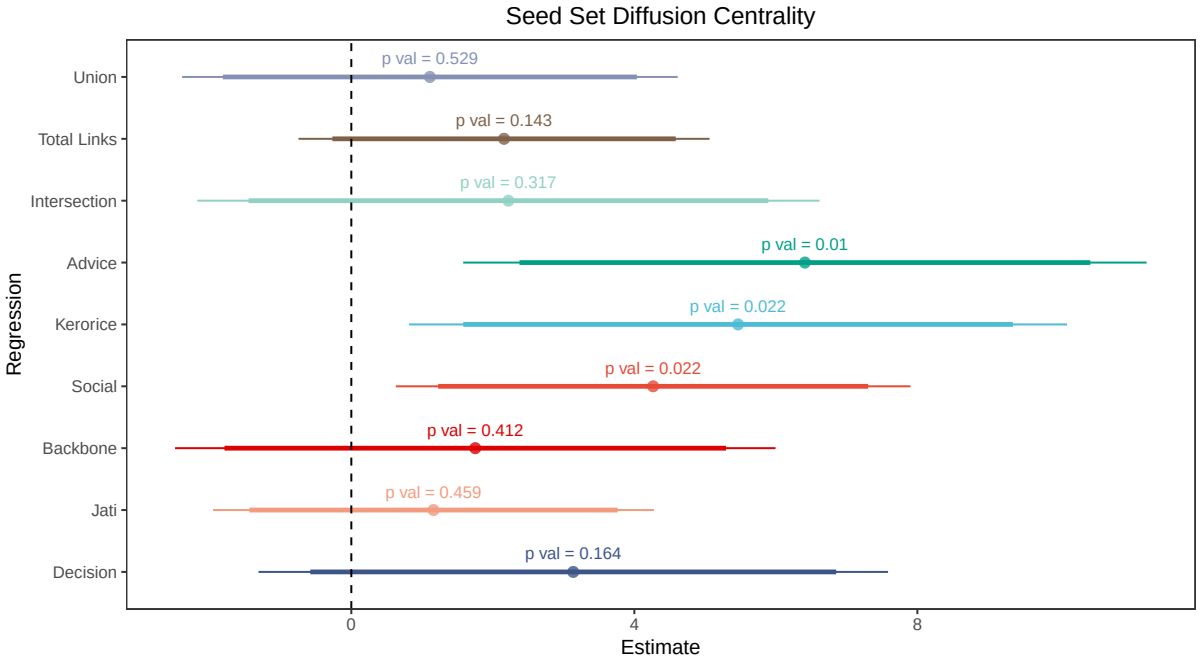

FIGURE S1. OLS Estimates for Impact of Seed Set Diffusion Centrality

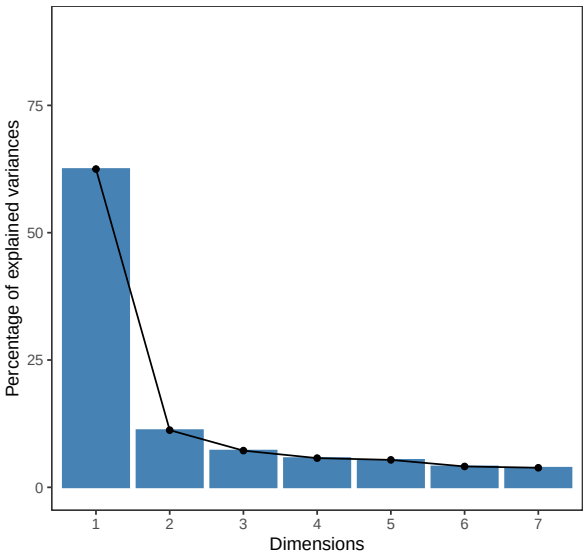

(A) Scree Plot: Microfinance Villages

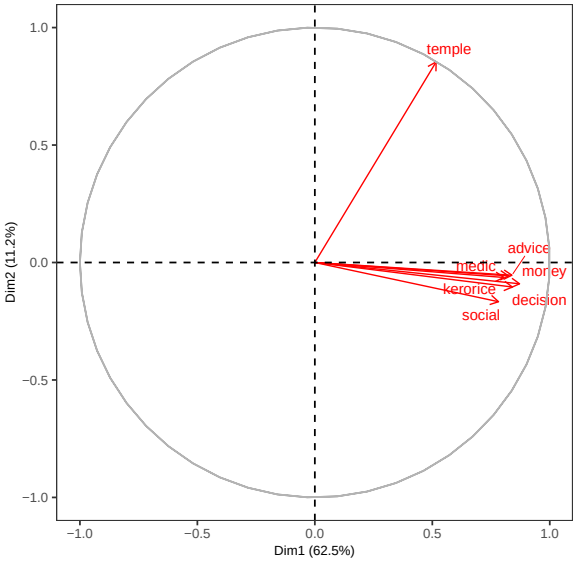

(B) Principal Components: Microfinance Villages

FIGURE S2. Principal Component Analysis with the Temple Layer, but without Geography or Jati layers.

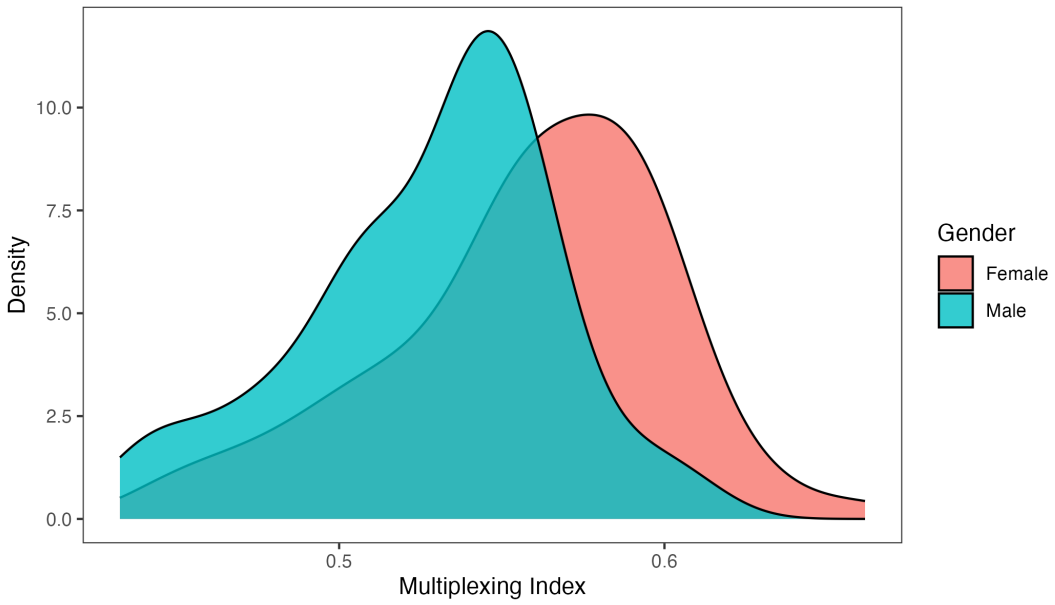

FIGURE S3. Multiplexing by gender.

Here we redo the analysis from Figure 8, but instead using the individual network data from Microfinance villages collected as part of Wave I of data collection in Banerjee et al. (2013) (instead of Wave II).[21]

[21]We have individual-level gender-distinguished data in the Wave I network survey, which elicited links from 46% of the households, giving us information on 70.84% of the links.

A.2. **Supplementary Tables.** In Table S1, we redo Table 2 but with the aggregate networks of union, intersection, and backbone constructed without including jati (the total link network is directed and never included jati).

TABLE S1. Seed Set Diffusion Centrality (Jati excluded from aggregate layers)

	No. Calls Received								
	1	2	3	4	5	6	7	8	9
Social	4.266								
	(1.820)								
	[0.022]								
Kero/Rice		5.466							
		(2.326)							
		[0.022]							
Advice			6.410						
			(2.416)						
			[0.010]						
Decision				3.137					
				(2.226)					
				[0.164]					
Jati					1.161				
					(1.559)				
					[0.459]				
Union						2.868			
						(1.994)			
						[0.155]			
Intersection							4.492		
							(1.996)		
							[0.028]		
Backbone								5.851	
								(2.575)	
								[0.027]	
Total Links									2.158
									(1.453)
									[0.143]
Num.Obs.	68	68	68	68	68	68	68	68	68
R2	0.194	0.254	0.313	0.161	0.110	0.145	0.227	0.263	0.131
Dep Var mean	8.691	8.691	8.691	8.691	8.691	8.691	8.691	8.691	8.691

Note: Robust standard errors are given in parentheses and p-values in square brackets. Controls added: number of households, its powers, and a dummy for number of seeds in the village. Exogenous variables are the sum of Diffusion Centrality for seeds in each village for the layer. Exogenous variables have been standardized. None of the aggregate layers (union, intersection, backbone and total links) uses jati as an input.

TABLE S2. Component Loadings: Microfinance Villages

Network	PC1	PC2	PC3	PC4	PC5	PC6	PC7	PC8	PC9
social	0.37	-0.04	-0.03	0.18	-0.55	0.69	-0.13	-0.17	-0.07
kerorice	0.38	0.02	0.01	0.07	-0.43	-0.69	-0.38	-0.17	-0.11
money	0.41	0.06	0.02	0.11	0.07	0.01	-0.14	0.72	0.52
advice	0.40	0.08	0.03	0.07	0.51	0.11	-0.22	0.16	-0.70
decision	0.40	0.07	0.02	0.12	0.47	0.03	-0.01	-0.62	0.45
medic	0.39	0.05	0.01	0.07	-0.12	-0.17	0.88	0.04	-0.14
temple	0.24	0.06	0.02	-0.96	-0.05	0.08	-0.02	-0.03	0.03
jati	0.10	-0.66	-0.74	-0.04	0.08	-0.04	0.01	0.02	0.00
distance	-0.07	0.73	-0.68	0.02	-0.05	0.01	-0.02	-0.01	0.00

TABLE S3. Component Loadings: RCT Villages

Network	PC1	PC2	PC3	PC4	PC5
social	0.49	0.03	-0.58	0.52	-0.39
kerorice	0.50	0.04	-0.39	-0.48	0.60
advice	0.50	0.05	0.37	-0.51	-0.59
decision	0.49	0.05	0.61	0.50	0.37
jati	0.09	-1.00	0.02	0.00	0.00

TABLE S4. F-test for the layers

layer	df	R.sq.	F-stat	p-val	F-stat marginal	p-val marginal
Advice	1	0.233	20.057	0.000		
Jati	2	0.263	2.628	0.110	2.628	0.110
Decision	3	0.272	1.728	0.186	0.834	0.365
Kero/Rice	4	0.293	1.768	0.162	1.804	0.184
Social	5	0.293	1.306	0.278	0.006	0.938

A.3. **Algorithms.** ..

Algorithm 1: Diffusion Simulation on Multiplexed Networks

Input: Multiplexed network's adjacency matrix $G = \{G^{(1)}, G^{(2)}\}$, transmission probability q, infection threshold τ, recovery probability δ, initial set of infected nodes I_0

Output: Share of infected nodes in steady state

Definitions:

- N: Set of all nodes in the network, $|N| = n$
- S_t: Set of susceptible nodes at time t
- I_t: Set of infected nodes at time t
- $\sigma_{i,t}$: State of node i at time t, where $\sigma_{i,t} \in \{S, I\}$
- $E_{i,t}$: Number of exposures (infections) node i is exposed to at time t

Step 1: Initialize $S_0 = N \setminus I_0$, I_0;

Step 2: **while** $t <$ *1000* **do**

  foreach $i \in S_t$ **do**

    Calculate $E_{i,t} = \sum_{j \in N} \sum_{l=1}^{2} G_{ij}^{(l)} \cdot \mathbb{I}(\sigma_{j,t} = I) \cdot q$;

    if $E_{i,t} \geq \tau$ **then**

      Node i becomes infected: $\sigma_{i,t+1} = I$;

    end

  end

  foreach $i \in I_t$ **do**

    Node i recovers with probability δ: $\sigma_{i,t+1} = S$ with probability δ;

  end

  Update $S_{t+1} = \{i \in N \mid \sigma_{i,t+1} = S\}$;

  Update $I_{t+1} = \{i \in N \mid \sigma_{i,t+1} = I\}$;

  if $abs(\frac{|I_{t+1}|}{n} - \frac{|I_t|}{n}) < 1e-8$ **then**

    break;

  end

end

Step 4: After convergence, run the simulation for an additional 100 iterations to stabilize the results and take the average across these iterations;

Algorithm 2: Multiplexed Network Generation

Input: Three network layers represented as adjacency matrices: A_1, A_2, A_3

Output: Two multiplexed networks M_1 and M_2

Step 1: Use `keroricego`, `visitgo`, and `advice` as the three matrices respectively;

Step 2: Sort A_2 and A_3 based on their average out-degree, in descending order;

Step 3: Prune the network with the higher average out-degree (among A_2 and A_3) to match that of the network with the lower average out-degree. Denote the pruned network as A_2';

Step 4: Generate the first multiplexed network, M_1, by combining the adjacency matrices of A_1 and the unpruned network (either A_2 or A_3, whichever had the lower out-degree);

Step 5: Generate the second multiplexed network, M_2, by combining the adjacency matrices of A_1 and A_2';